Coordination Chemistry Reviews 436 (2021) 213773

Contents lists available at ScienceDirect

Coordination Chemistry Reviews

journal homepage: www.elsevier.com/locate/ccr

Review

Electrochemistry of Ru(edta) complexes relevant to small molecule transformations: Catalytic implications and challenges

Debabrata Chatterjee [a,b,*], Maria Oszajca [c], Anna Katafias [d], Rudi van Eldik [b,c,d,*]

[a] Vice-Chancellor's Research Group, Zoology Department, University of Burdwan, Burdwan 713104, India
[b] Department of Chemistry and Pharmacy, University of Erlangen-Nuremberg, Egerlandstr. 1, 91058 Erlangen, Germany
[c] Faculty of Chemistry, Jagiellonian University, Gronostajowa 2, 30-387 Krakow, Poland
[d] Faculty of Chemistry, Nicolaus Copernicus University in Torun, Gagarina 7, 87-100 Torun, Poland

ARTICLE INFO

Article history:
Received 20 October 2020
Accepted 3 January 2021

Keywords:
Ru(edta)
Electrochemistry
Mononuclear complexes
Binuclear complexes
Small molecule activation

ABSTRACT

Electrochemistry of Ru(edta) complexes ($edta^{4-}$ = ethylenediaminetetraacetate) progressed over a period of several decades, with significant increase in understanding of the electro-catalytic processes involving the substrate coordinated to the metal center. While electrochemistry studies of many Ru(edta) complexes were published in several papers, no attempt has been made to provide a comprehensive and systematic overview of its electrochemical properties, evaluating its application to catalytic electrochemical transformation of small molecules. In this article, results of the electrochemical studies of both mononuclear and binuclear complexes of Ru(edta) are reviewed with regard to electron-transfer reaction mechanism and activity. Their potential to act as redox mediators or catalysts in electrochemical transformations of small molecules and enzymatic reactions, are highlighted. This review aims to contribute to the mechanistic understanding of Ru(edta) complexes in catalysis of such electrochemical transformations.

Contents

* Corresponding authors at: Department of Chemistry and Pharmacy, University of Erlangen-Nuremberg, Egerlandstr. 1, 91058 Erlangen, Germany.
E-mail addresses: dchat57@hotmail.com (D. Chatterjee), rudi.vaneldik@fau.de (R. van Eldik).

https://doi.org/10.1016/j.ccr.2021.213773
0010-8545/

1. Introduction

Small molecules whose activation and transformations are of continued interest include O_2, H_2O, H_2O_2, H_2, N_2, NO, NO_2^-, CO_2 and H_2S [1–10]. Chemical transformations of these molecules, viz. reduction of N_2 or NO_2^- to NH_3, reduction of CO_2 to HCOOH/CH_3OH, reduction of O_2 to H_2O_2, H_2 evolution reaction (HER) and oxidation of H_2O to O_2, are of great concern mostly in the area of environment and energy. It may be noted here that all the aforesaid reactions occur in nature, and are catalyzed by active sites of metalloenzymes. Synthesis of coordination compounds of metal ions as 'small-molecule models' of such metalloenzymes, and their application to mimic the above referred enzymatic transformations of small molecules effectively, has become a challenging area of research. Apart from the ligand design that integrates the structural characteristics found at the active sites of the enzymes, electrochemical behavior of such biomimetic compounds is another key-factor that governs their capability to act as redox mediators and/or oxidative catalysts in achieving the aforementioned small-molecule transformations in resemblance to the enzymatic reactions.

The Ru(edta) complexes meet the basic requirements apposite to a model that mimic 'small-molecule' activation of metalloenzymes. The ability of the 'edta' ligand ($edta^{4-}$ = ethylenediaminete traacetate) to act as a multi-dentate ligand with its carboxylate and amine donors are comparable to that of the metalloenzymes. Another noteworthy aspect, the water molecule in $[Ru^{III}(edta)(H_2O)]^-$ is highly active towards substitution reactions similar to rapidly interchangeable water molecules located in the active sites of such metalloenzymes [11]. Though the chemistry of $[Ru(edta)(H_2O)]^-$ is dominated by its lability towards aqua-substitution reactions, the upsurge in interest in studying the electrochemistry of Ru(edta) complexes appeared in the early seventies. Studies concerning reactivity of the $[Ru^{III}(edta)(H_2O)]^-$ complex emphasizing its prospect in bio-inorganic applications, have been adequately reviewed before [11–15]. However, this article for the first time systematically reviews the electrochemical properties of Ru(edta) complexes with the aim of evaluating their ability in mediating small-molecule transformations electrochemically. The '$Hedta^{3-}$' in the $[Ru^{III}(Hedta)(H_2O)]$ complex acts as a penta-coordinating ligand (Fig. 1) [16,17]. The metal complex is stable in aqueous solution, however, with the increase in pH of the solution, deprotonation of the dangling carboxylic acid group (pK_{a1} = 2.4) and the coordinated water molecule (pK_{a2} = 7.6) occurs successively [18,19] as shown in Scheme 1.

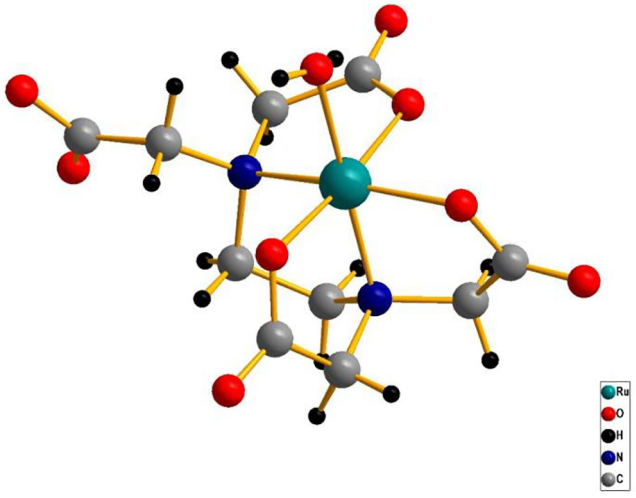

Fig. 1. 3D crystal structure of the $[Ru^{III}(Hedta)(H_2O)]$ complex.

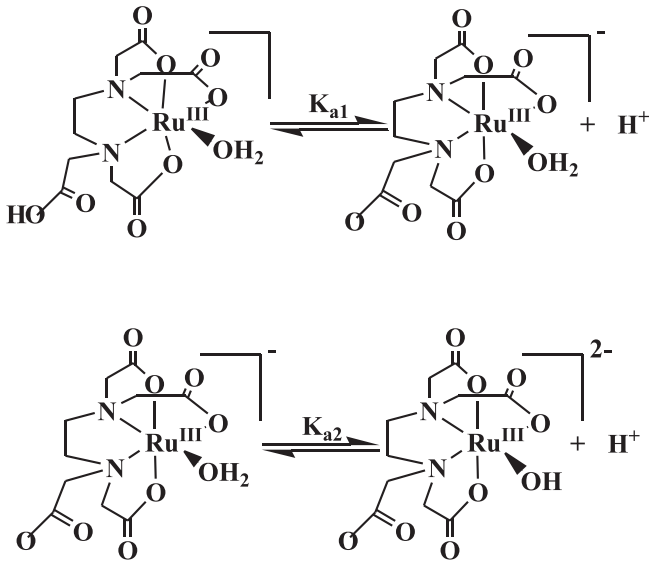

Scheme 1. Acid-dissociation equilibria of $[Ru^{III}(Hedta)(H_2O)]$

The $[Ru^{III}(edta)(H_2O)]^-$ complex is highly reactive towards aqua-substitution reactions in the pH range 4–6 [11]. The $[Ru^{III}(edta)(H_2O)]^-$ in water is almost featureless over the entire visible range of the spectrum, but exhibits a strong absorption band in the UV region (λ_{max} = 284 nm). The Ru(II) analogue, $[Ru^{II}(edta)(H_2O)]^{2-}$ displays almost similar spectral features exhibiting an intense band at 282 nm [18].

2. Electrochemistry of Ru^{III}(edta) complexes

During the 1970's, the electrochemical behavior of the $[Ru^{III}(Hedta)(H_2O)]$ complex was examined both with polarographic and voltammetric techniques at a mercury electrode as a function of pH [20,21]. The half-wave potential corresponding to a diffusion controlled polarographic step attributed to the one-electron reduction of $[Ru^{III}(Hedta)(H_2O)]$ to $[Ru^{II}(Hedta)(H_2O)]^-$ was found to be more negative with increasing pH [20] and tended to reach a limiting value at a pH higher than 5.0. This reduction step was found to be DC-polarographically reversible in the pH range 3–5. The pH dependency of the $E_{1/2}$ values corresponding to the Ru^{III}/Ru^{II} redox couple, was explained in terms of the proton dissociation of the uncoordinated –COOH group as shown in Scheme 2. At higher pH (>6) lack of reversibility was noticed because of the considerable difference in the proton-dissociation equilibrium (Scheme 2) values of $[Ru^{III}(edta)(H_2O)]^-$ (pK_{a2} = 7.6) and $[Ru^{II}(edta)(H_2O)]^{2-}$ (pK'_{a2} > 10) complexes [20].The analogous pH dependence of the formal potential corresponding to the Ru^{III}/Ru^{II} redox couple, determined from the average of the anodic and cathodic peak potentials in cyclic voltammograms, was also noticed by Anson and co-worker [21].

Later studies [18] further revealed that the reversibility of the reactions at the electrode diminished in the following order: HDME (hanging drop mercury electrode) > PBE (platinum button electrode) > PGE (pyrolytic graphite electrode). The cyclic voltammogram of the $[Ru^{III}(edta)(H_2O)]^-$ complex performed at HDME as working electrode (in acetate buffer), was found to be quasi-reversible at pH 5.5 with a ΔE_p value of 70 mV (separation between anodic and cathodic peaks) [18] and the formal potential ($E_{1/2}$) associated with the Ru^{III}/Ru^{II} couple in $[Ru^{III}(edta)(H_2O)]^-$ was reported to be −0.01 V (vs. SHE) [18].

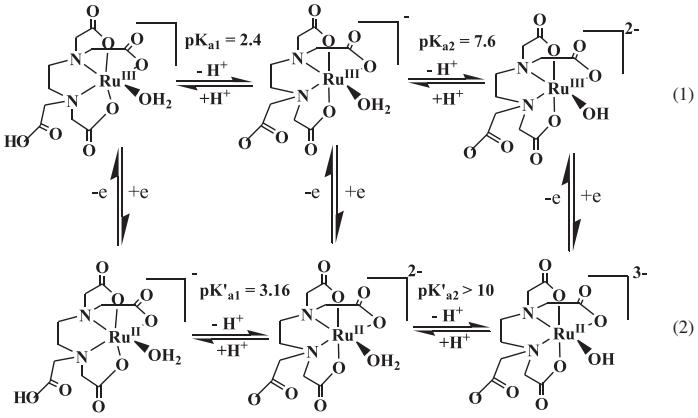

Scheme 2. Electrode reactions and proton dissociation equilibria of $[Ru^{III/II}(Hedta)(H_2O)]^{0/-}$ complexes.

Formation of oxo-bridged dimeric mixed-valence species, $[(edta)Ru^{IV}\text{-}O\text{-}Ru^{III}(edta)]$, was noticed during electrochemical studies of $[Ru^{III}(edta)(H_2O)]^-$ in aqueous solution of sodium chlorate [22]. This Ru(IV)-Ru(III) dimer complex could be reduced at the mercury electrode to Ru(III)-Ru(III) species, which subsequently decomposed to the Ru(III)-monomer complex [22]. Noteworthy here, is that the formation of a polarographically inactive $[Ru^{II}(edta)(CO)]^{2-}$ complex was reportedly observed when the reduction of $[Ru^{III}(edta)(H_2O)]^-$ in the formate buffer solution (sodium formate/formic acid solution) was conducted at the mercury electrode [23].

2.1. Electrochemistry of the $[Ru^{III}(edta)(H_2O)]^-$ complex immobilized on a solid surface

Anson et al. explored the procedure for attaching Ru(edta) complexes to the graphite electrode [21] in order to exploit electrocatalysis of such complexes. The process of attaching $[Ru^{III}(Hedta)(H_2O)]$ to a graphite electrode involved the coupling of the uncoordinated carboxylic acid group (–COOH) in the $[Ru^{III}(Hedta)(H_2O)]$ complex with the pre-incorporated amine groups at the surface of the graphite electrode [21]. The linkage between the metal complex and the electrode was established through an amide bond formed by condensation of the pendant carboxylic acid of the metal complex with the amine group pre-attached to the electrode [21]. Results of the ligand substitution reaction carried out with Ru(edta) complexes attached to the graphite electrode surface, revealed that only $[Ru^{II}(edta)(H_2O)]^{2-}$ was efficacious towards aqua-substitution, but not its Ru(III) analogue [21]. The water molecule in the surface attached $[Ru^{II}(edta)(H_2O)]^{2-}$ complex could be readily displaced by the substituting ligands, L (L = pyridine, isonicotinamide and nicotinamide) [21]. The difference in the reactivity between the attached and unattached complexes may be explicable with regard to the labilizing effect of the uncoordinated dangling carboxylate group in the $[Ru^{III}(edta)(H_2O)]^-$ complex. While the pendent carboxylate group in the unbound $[Ru^{III}(edta)(H_2O)]^-$) complex was shown to be responsible for labilization of the $Ru^{III}\text{-}OH_2$ bond [11,18,19] the same effect is not rendered possible in case of the surface bound $[Ru^{III}(edta)(H_2O)]^-$ complex because of the engagement of the dangling carboxylate group to form an amide bond for tethering the metal complex and the electrode surface together, and the complex becomes substitution inert as observed [21].

Anchoring the $[Ru^{III}(Hedta)(H_2O)]$ complex to the graphite electrode without involving the uncoordinated carboxylic acid group, is also available in the literature [24]. A graphite electrode pretreated with 4-methylaminopyridine to produce $–CONHCH_2C_5H_4N$,

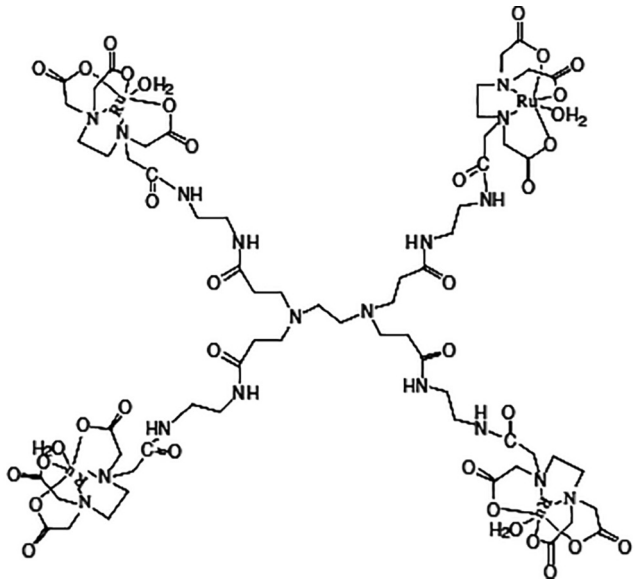

Fig. 2. Schematic presentation of the PAMAM dendrimer bound $[Ru^{III}(edta)(H_2O)]^-$ complex. Reproduced from Ref. [31].

was used for this purpose and the $[Ru^{III}(edta)(H_2O)]^-$ complex was attached to the surface by coordination of the pyridine moiety of the graphite bound ligand directly to the Ru(III) center [24]. A most intriguing fact of the study, is that despite the attached Ru(III) complex contained the pendent carboxylate group, it showed a much lower reactivity towards ligand substitution reactions as compared to that reported for the unattached $[Ru^{III}(edta)(H_2O)]^-$ complex in homogeneous solution [18,19,25]. The results of the above studies [21,24] taken together, point to the fact that the lability of the $[Ru^{III}(edta)(H_2O)]^-$ complex towards substitution is considerably lower when the metal complex is surface bound through its pendent carboxylate group.

The immobilization of the $H[Ru^{III}(H_2edta)Cl_2]$ complex [26] on to the surface of silica gel modified with [3-(2-aminoethyl)amino propyl]trimethoxysilane (SF-AEATS), was achieved by the condensation of the pendent carboxylate group of the metal complex with amine groups present in SF-AEATS [27]. However, the aforementioned immobilization of the precursor, $H[Ru^{III}(H_2edta)Cl_2]$ resulted in the formation of the surface anchored dimeric SF-AEATS-$[(edta)_2Ru_2(IV,IV)]$ complex [27]. It was further reported that the SF-AEATS-$[(edta)_2Ru_2(IV,IV)]$ complex could affect oxidation of H_2O to O_2 with concurrent formation of the SF-AEATS-

[(edta)$_2$Ru$_2$(III$_{1/2}$,III$_{1/2}$)] complex possessing the formal oxidation state of each metal atom as '+3.5' [27]. It may be noted that Anson et al. [28] reported that the electrochemical oxidation of [Ru^{III}(edta)(H$_2$O)]$^-$ resulted in the formation of an oxo- or a dihydroxo bridged [(edta)$_2$Ru$_2$(III$_{1/2}$,III$_{1/2}$)] species. The same species upon exposure to NO gas produced the monomeric, SF-AEATS bound [Ru^{II}(edta)(NO$^+$)]$^-$ complex [29]. Cyclic voltammetric studies of the bound complex was performed, and the $E_{1/2}$ value (−0.09 V vs. SHE [29]) for the SF-AEATS-[Ru^{II}(edta)(NO$^+$)]$^-$/SF-AEATS-[Ru^{II}(edta)(NO^0)]$^{2-}$ couple was found to be very close to the $E_{1/2}$ value (−0.07 V vs. SHE) reported for the Ru^{III}/Ru^{II} couple for the unbound complex [30].

Later the same group explored the possibility of anchoring the [Ru^{III}(Hedta)(H$_2$O)] complex on poly(amidoamine) dendrimers (PAMAM) [31]. The metal complex was tethered with the dendrimers through peptide bonds (Fig. 2) formed in the reaction of the uncoordinated carboxylic acid arm of the metal complex and the terminal amine groups of the dendrimers [31]. Cyclic voltammograms of the anchored complex showed a pair of reversible waves assigned to the metal-based one electron transfer reaction at the electrode, and the formal potential (0.04 V vs. SHE) for the Ru$^{III/II}$ couple is very close to the value (0.01 V vs. SHE) observed for the unbound complex [31]. The reported results are suggestive of the fact that the electrochemical properties of the dendrimer bound [Ru^{III}(edta)(H$_2$O)]$^-$ complex are not appreciably altered in comparison to its free form [31]. Further to this, the dendrimer bound [Ru^{III}(edta)(H$_2$O)]$^-$ complex upon exposure to NO gas converted into [Ru^{III}(edta)(NO)]$^-$. Electrochemical properties of the PAMAM dendrimer bound [Ru^{II}(edta)(NO$^+$)]$^-$ complex were evaluated by cyclic voltammetric studies, and the reported $E_{1/2}$ value (-0.08 V vs. SHE) for the NO$^+$/NO^0 couple was found to be comparable with the value reported for the unbound [Ru^{II}(edta)(NO$^+$)]$^-$ complex [30].

Immobilization of [Ru^{III}(edta)(H$_2$O)]$^-$ on the thin-film graphite electrodes surface using poly(4-vinylpyridine) (PVP) coats was also achieved by Anson et al [32] and cyclic voltammetric responses of the attached metal complex was found to be agreeable to the occurrence of a reversible redox reactions [32].

Table 1
Formal potentials ($E_{1/2}$) for Ru^{III}/Ru^{II} couple in [Ru^{III}(edta)(L)]$^-$

Mono-dentate ligand (L)	[a] $E_{1/2}$ (V vs. SHE)	Refs.
Water	−0.01	[18]
Pyridine	0.10	[18]
Imidazole	0.10	[18]
Benzimidazole	−0.01	[35]
Benzotriazole	0.10	[35]
Isonicotinamide	0.16	[18]
Pyrazine	0.24	[18]
Acetonitrile	0.26	[18]
Thiocyanate	0.07	[18]
Nicotinamide	0.16	[21]
Adenine	0.12	[36]
Adenosine	0.09	[36]
Cytosine	−0.03	[36]
Cytidine	−0.03	[36]
Thymine	−0.02	[36]
Guanosine	0.03	[37]
Inosine	0.07	[37]
Xanthosine	0.06	[37]
Uracil	−0.23	[38]
Hypoxanthine	0.07	[39]
Carbon monoxide (CO)	−0.01	[40]
Triphenylphosphene (PPh$_3$)	0.13	[41]
Nitric oxide (NO)	−0.11	[30]
Chloride (Cl$^-$)	0.00	[22]
Azide (N_3^-)	−0.08	[42]
Dimethylsulfide (DMS)	0.12	[43]
Dimethylsulfoxide (DMSO)	0.56	[44]

[a] Potentials are converted into SHE where reported with different reference electrodes.

2.2. Electrochemistry of the Ru(edta) complexes containing monodentate co-ligands

The [Ru^{III}(edta)(H$_2$O)]$^-$ complex readily reacts with a myriad of incoming ligands, L (L = monodentate ligands) to form [Ru^{III}(edta)(L)]$^-$ complexes (charge on the substituting mono-dentate ligands, L is dropped for the sake of convenience) through a straightforward water displacement reaction (Eq. (3)).

$$\left[Ru^{III}(edta)(H_2O)\right]^- + L \rightarrow \left[Ru^{III}(edta)(L)\right]^- + H_2O \quad (3)$$

Redox properties of many such [Ru^{III}(edta)(L)]$^-$ complexes were electrochemically examined, and most of them showed reversible metal based electron transfer (Eq. (4)).

$$\left[Ru^{III}(edta)(L)\right]^- \underset{-e}{\overset{+e}{\rightleftharpoons}} \left[Ru^{II}(edta)(L)\right]^{2-} \quad (4)$$

The values of the formal potential reported for the [Ru^{III}(edta)L]$^-$/[Ru^{II}(edta)L]$^{2-}$ couple are tabulated in Table 1 for the purpose of assessing how the nature of the ligands L influences the redox chemistry of the [Ru^{III}(edta)(L)]$^-$ complexes. It may be noted that the [Ru^{III}(Hedta)(NO)] complex exhibited ligand based (L = NO) electron transfer [30] as shown in Scheme 3.

Noteworthy here, is that while [Ru^{II}(Hedta)(NO$^+$)] undergoes a ligand-based electron transfer process (Scheme 3), a metal based electron-transfer reaction at the electrode was reported for the [Ru^{III}(Hedta)(NO$^+$)]$^+$ complex (prepared by reacting [Ru^{III}(Hedta)(H$_2$O)] with NOBH$_4$) [33]. The $E_{1/2}$ value (estimated by cyclic voltammetry) reported for the Ru^{III}/Ru^{II} redox couple in [Ru^{III}(Hedta)(NO$^+$)]$^+$ is −0.07 V (vs. SHE) [33]. The above difference in the electrochemical behavior of [Ru^{III}(Hedta)(NO$^+$)]$^+$ and [Ru^{II}(Hedta)(NO$^+$)], is clearly suggestive of the fact that the NO$^+$ in the [Ru^{III}(Hedta)(NO$^+$)]$^+$ complex is less electrophilic than in the [Ru^{II}(Hedta)(NO$^+$)] complex.

Toma and co-workers [34,35] examined the pH dependence of the electrochemical properties of the Ru(edta) complexes comprising benzotriazole (Hbta) and benzimidazole (Hbim) ligands (Fig. 3). Cyclic voltammetric examination of the [Ru^{III}(edta)(Hbta)]$^-$ complex performed at different pH, revealed that the $E_{1/2}$ value associated with the [Ru^{III}(edta)(Hbta)]$^-$/[Ru^{II}(edta)(Hbta)]$^{2-}$ redox couple systematically shifted from the value 0.13 V (vs. SHE) to −0.04 V (vs. SHE) by increasing the pH values from 3 to 10, respectively [34]. The [Ru^{III}(edta)(Hbim)]$^-$ complex also exhibited a similar trend with regard to the pH dependence of the $E_{1/2}$ values, which signifies that both the complexes undergo one-proton coupled one-electron redox reactions [35].

$$[Ru^{III}(Hedta)(NO)] \longleftrightarrow [Ru^{II}(Hedta)(NO^+)] \quad (5)$$

$$[Ru^{II}(Hedta)(NO^+)] \xrightarrow[-0.07V\ (vs.SHE)]{+e,\ pH = 1.2} [Ru^{II}(Hedta)(NO^0)]^- \quad (6)$$

Scheme 3. Electron transfer reactions of the nitrosyl [Ru^{III}(Hedta)(NO)] complex.

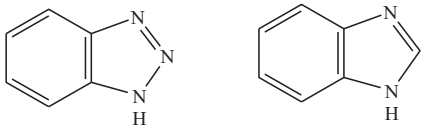

Benzotriazole (Hbta) Benzimidazole (Hbim)

Fig. 3. Schematic presentation of the benzotriazole and benzimidazole ligands.

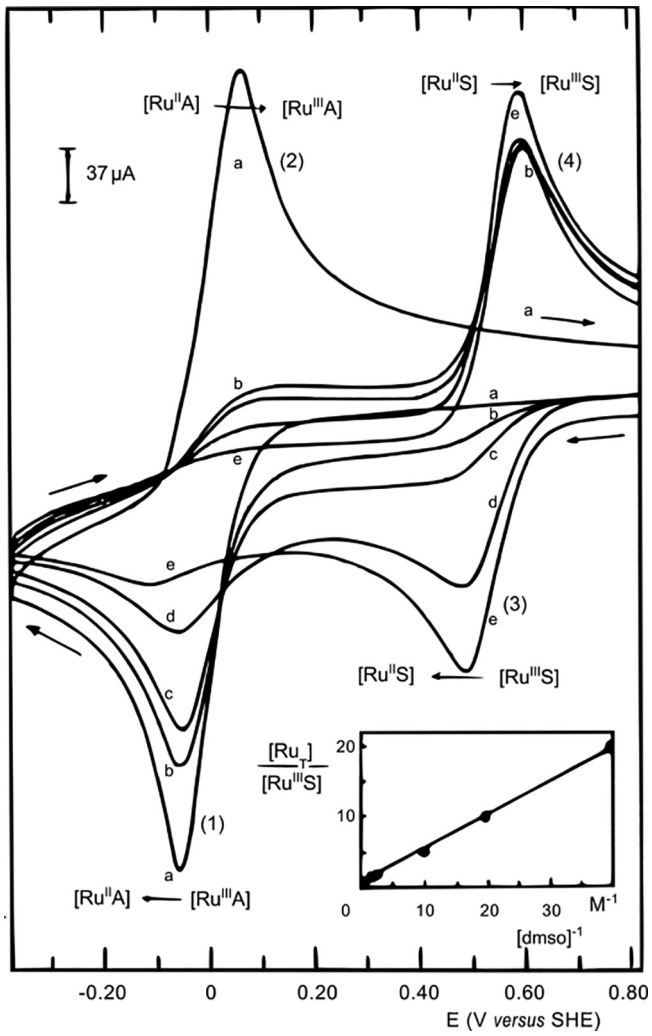

Fig. 4. Cyclic voltammograms of the $[Ru^{III}(edta)(H_2O)]^-$ (designated as $[Ru^{III}A]$) and S-bonded $[Ru^{III}(edta)(DMSO)]^-$ (designated as $[Ru^{III}S]$) complexes (5 mM) in the presence of [DMSO] = 0 (a), 0.050 (b), 0.10 (c), 0.50 (d) and 2.0 M (e); pH 4.5 (acetate buffer), T = 25 °C; scan rate 200 mV s^{-1}; Inset: linear plot of $[Ru_T]/[Ru^{III}S]$ vs. 1/[DMSO]. Reproduced from Ref. [44].

$$[Ru^{III}(edta)(H_2O)]^- + DMSO \underset{}{\overset{K^{Ru(III)-S}}{\rightleftharpoons}} [Ru^{III}(edta)(DMSO)]^- + H_2O$$
$$(Ru^{III}A) \qquad\qquad (Ru^{III}S)$$
$$\updownarrow -0.01V \qquad\qquad \updownarrow 0.56V$$
$$[Ru^{II}(edta)(H_2O)]^{2-} + DMSO \underset{}{\overset{K^{Ru(II)-S}}{\rightleftharpoons}} [Ru^{II}(edta)(DMSO)]^{2-} + H_2O$$
$$(Ru^{II}A) \qquad\qquad (Ru^{II}S)$$

Scheme 4. Schematic representation of electrochemical redox reactions of $[Ru^{III/II}(edta)(H_2O)]^{-/2-}$/$[Ru^{III/II}(edta)(DMSO)]^{-/2-}$

It is of interest to discuss the electrochemistry of the dimethylsulfoxide (DMSO) complexes of Ru(edta) in detail. It had been reported that the $[Ru^{III}(edta)(H_2O)]^-$ (designated as $[Ru^{III}A]$) reacts with excess DMSO to form the S-bound $[Ru^{III}(edta)(DMSO)]^-$ (designated as $[Ru^{III}S]$) [45]. The formation of the O-bound $[Ru^{III}(edta)(DMSO)]^-$ (designated as $[Ru^{III}O]$) complex, is not favored thermodynamically as indicated by the very small value of the isomerization constant (K_i = $[Ru^{III}O]/[Ru^{III}S]$ = 0.03) [44] and therefore, the formation of $Ru^{III}O$ species in the reaction system is negligibly small.

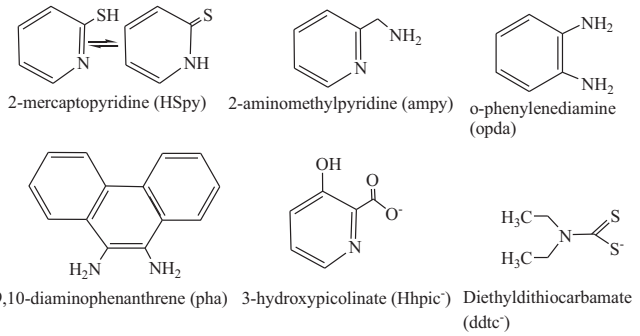

Fig. 5. Schematic presentation of the bidentate ligands used by Toma and coworkers (Ref. [45–50]).

$$\underset{(Ru^{III}A)}{\left[Ru^{III}(edta)(H_2O)\right]^-} + DMSO \overset{K^{Ru(III)-S}}{\rightleftharpoons} \underset{(Ru^{III}S)}{[Ru(edta)(DMSO)]^-} + H_2O \qquad (7)$$

Due to the poor nucleophilicity of the ligand, the $[Ru^{III}S]$ complex is thermodynamically unstable ($K^{Ru(III)-S}$ = 1.8 M^{-1} [44]), undergoes reversible aquation, and exists in equilibrium with $[Ru^{III}(edta)(H_2O)]^-$ even at high concentrations of DMSO (Eq. (7)). Formation of the $[Ru^{III}S]$ complex was monitored by cyclic voltammetry [44]. In absence of DMSO, cyclic voltammograms of the solution of $[Ru^{III}(edta)(H_2O)]^-$ exhibited a pair of cathodic and anodic peaks for the electrochemical oxidation and reduction of $[Ru^{III/II}(edta)(H^2O)]^{-/2-}$ species. However, at high DMSO concentration, a new pair of waves appeared in the more positive potential range (Fig. 4). The formal potentials for the Ru^{III}/Ru^{II} couples in $[Ru^{III}A]^-$ and $[Ru^{III}S]^-$ appeared at −0.01 V and 0.56 V (vs. SHE), respectively [44]. While the cathodic peak corresponding to the reduction of $[Ru^{III}S]$ to $[Ru^{II}S]$, is seen only at high DMSO concentration (Fig. 4), the peak corresponding to the oxidation of $[Ru^{II}A]$ to $[Ru^{III}A]$ practically disappeared, whereas the peak currents relating to the oxidation of $[Ru^{II}S]$ to $[Ru^{III}S]$, attained a limiting value [44].

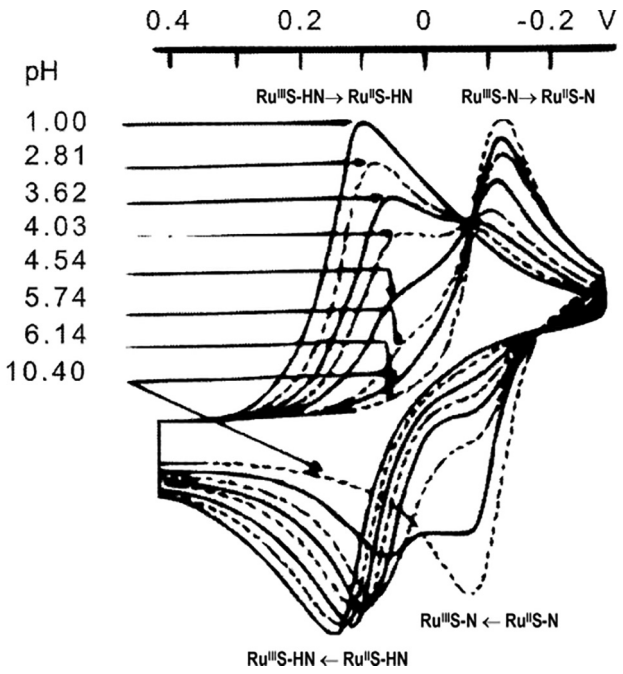

Fig. 6. Cyclic voltammograms of $Ru^{III/II}$(edta) complexes of 2-mercaptopyridine as a function of pH. Reproduced from Ref. [45].

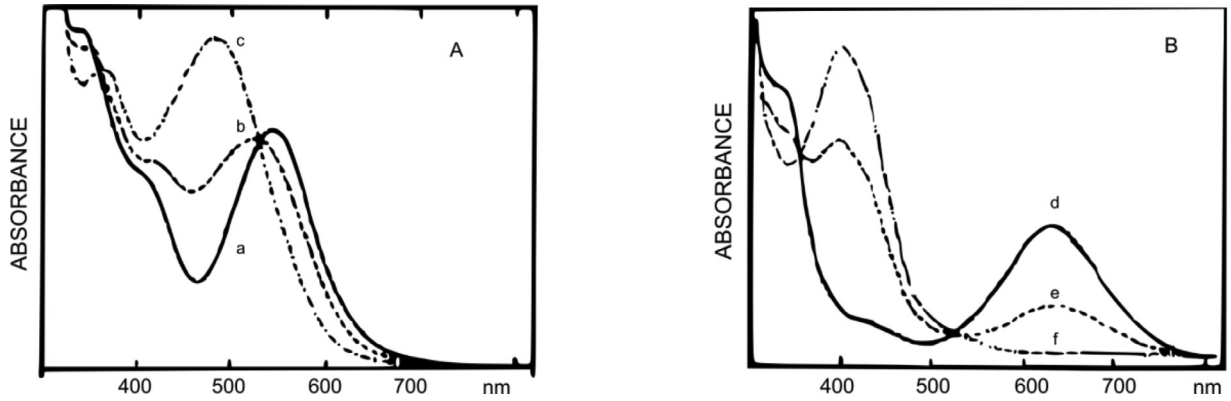

Fig. 7. Spectro-electrochemistry of $Ru^{III/II}$(edta) complexes of 2-marcaptopyridine at (A) pH = 2.8 and (B) pH = 9.2. Potentials applied (a) 0.22, (b) 0.3, (c) 0.42, (d) 0.12, (e) −0.13 and (f) −0.28 V (vs. SHE). Reproduced from Ref. [45].

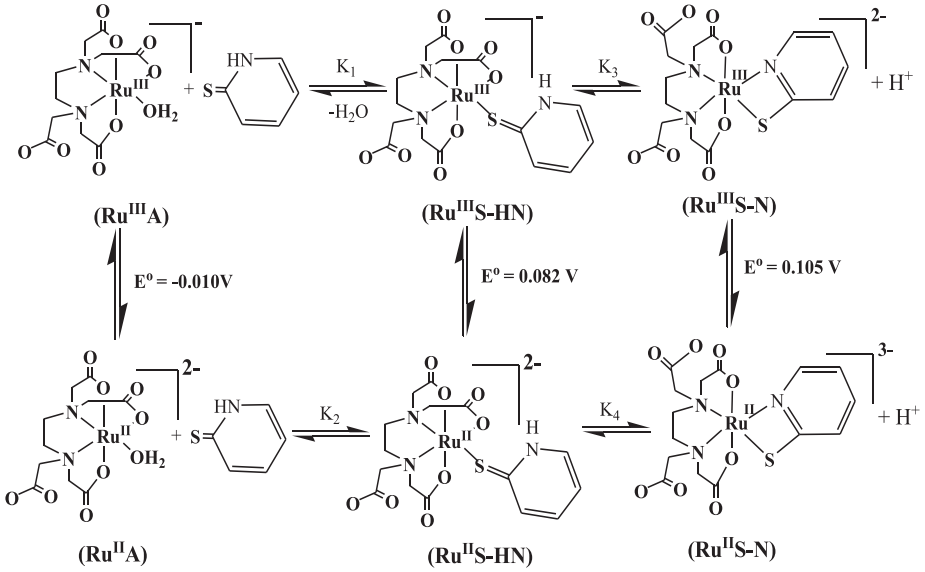

Scheme 5. Chelate formation reactions of $[Ru^{III/II}(edta)(H_2O)]^{-/2-}$ with the bidentate ligand, 2-mercaptopyridine.

The overall electrochemical observations as discussed above may be illustrated in Scheme 4. The values of the formation constants, $K^{Ru(III)-S}$ reported for [Ru^{III}S] and $K^{Ru(II)-S}$ for [Ru^{II}S] are 1.8 M^{-1} and 7.7 × 10^9 M^{-1}, respectively, [44] signifying the fact that the [Ru^{II}S] complex is highly stable thermodynamically as compared to its Ru(III) analogue.

2.3. Electrochemistry of the Ru(edta) complexes containing bidentate co-ligands

The electrochemistry of Ru(edta) complexes comprising the following bidentate co-ligands (Fig. 5) was studied by Toma and co-workers [45–50] and the results are discussed attaching particular importance to intra-molecular amine to imine rearrangement reactions.

The 2-mercaptopyridine ligand exists in tautomeric forms (Fig. 5) in aqueous solution. At pH < 3, the thione group of the ligand binds to ruthenium(III) center to form S-bound Ru(edta) complex of 2-mercaptopyridine, $[Ru^{III}(edta)(HSpy)]^-$ (denoted as Ru^{III}S-NH). The cyclic voltammograms (Fig. 5) of the [Ru^{III}S-NH] complex show only one pair of cathodic and anodic waves at pH < 3, which was attributed to the Ru^{III}/Ru^{II} redox couple in [Ru^{III}-S-NH] complex ($E_{1/2}$ = 0.134 V vs. SHE) [45]. Whereas, at higher pH (pH > 6) the $[Ru^{III}(edta)(HSpy)]^-$ complex converts into the mixed-chelate $[Ru^{III}(edta)(Spy)]^{2-}$ species (denoted as Ru^{III}S-N) displaying a pair of waves in the cyclic voltammogram (Fig. 6) associated with the Ru^{III}S-N/Ru^{II}S-N redox couple at $E_{1/2}$ = -0.103 V (vs. SHE) [45].

Spectral features of all the Ru(III)- and Ru(II)-complexes obtained from spectro-electrochemical studies, are shown in Fig. 7. While formation of an S-coordinated red complex, Ru^{III}S-HN (λ_{max} = 550 nm) is evident at lower pH, at higher pH (>6) the red complex turned into green (λ_{max} = 630 nm) due to formation of the chelated species, Ru^{III}S-N through the S and N donor atoms of the ligand [45]. Based on the results of electrochemical, spectro-electrochemical and other independent experiments, the following reaction Scheme 5 was proposed to illustrate the reaction of 2-mercaptopyridine with $[Ru^{III}(edta)(H_2O)]^-$ [45].

The reported values of the equilibrium constants, K_1, K_2, K_3 and K_4, are 3.1 × 10^6 M^{-1}, 1.1 × 10^8 M^{-1}, 4.5 × 10^{-5} M and 3.1 × 10^{-8} M, respectively [45]. Equilibrium constants values are suggestive of the fact that Ru^{II}S-NH species (Scheme 5) is comparatively more stable than its Ru(III) analogue. However, the Ru(II) chelated product Ru^{II}S-N (Scheme 5), is more vulnerable towards protonation than its Ru(III) analogue [45].

Noteworthy here, is that the mixed chelate complexes of Ru (edta) containing the bidentate ligand, 3-hydroxypicolinate

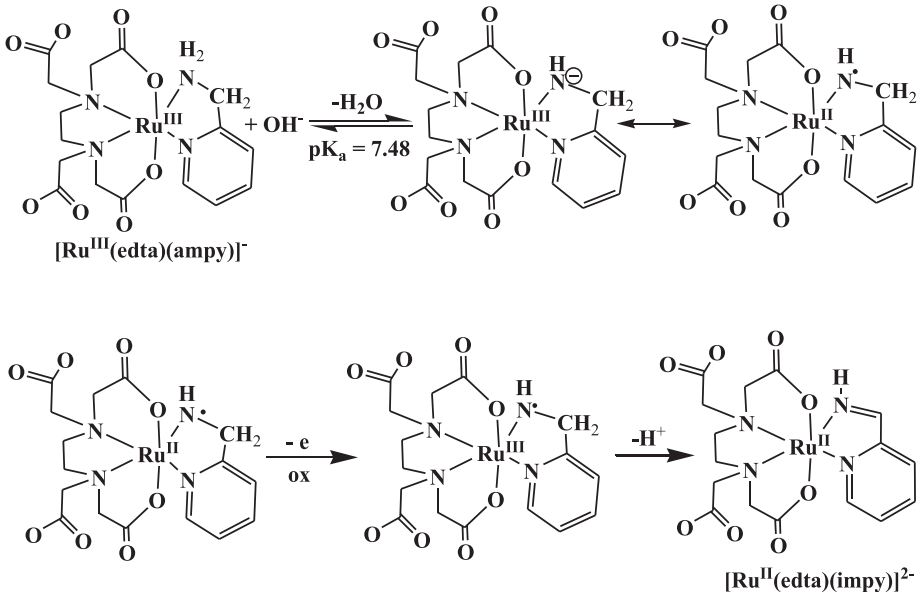

Scheme 6. Oxidative dehydrogenation of the ampy chelate in $[Ru^{III}(edta)(ampy)]^{-}$ forming $[Ru^{II}(edta)(impy)]^{2-}$

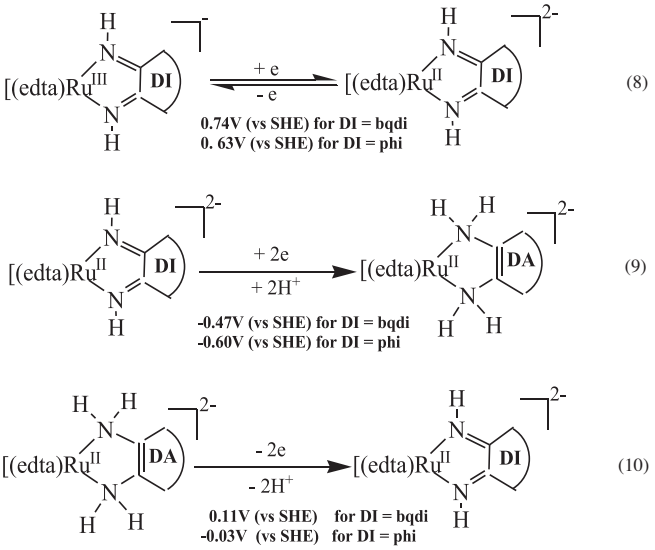

Scheme 7. Electrochemical redox reactions of di-imine (DI) complexes of Ru(edta) (bqdi = *ortho*-benzoquinone di-imine, phi = 9,10-phenanthrene quinone di-imine).

(Hhpic^{-}), revealed similar electrochemical behavior [46]. The $E_{1/2}$ value for the Ru^{III}/Ru^{II} couple in the $[Ru^{III}(edta)(Hhpic)]^{2-}$ complex was observed at 0.17 V (vs. SHE) at pH 4.7 [46]. It was further reported that in the pH range 4–8, the chelating ligand Hhpic^{-} coordinates to the Ru(III) center through its pyridine-N and carboxylate-O groups to form the $[Ru^{III}(edta)(\kappa\ N, \kappa\ O\text{-Hhpic})]^{2-}$ complex [46]. However, due to the fact that the phenolic OH group of the ligand (Hhpic^{-}) undergoes deprotonation at higher pH (>9), the $[Ru^{III}(edta)(\kappa\ N, \kappa\ O\text{-Hhpic})]^{2-}$ complex undergoes an intramolecular isomerization reaction to form $[Ru^{III}(edta)(\kappa\ O, \kappa\ O\text{-hpic})]^{3-}$, and the $E_{1/2}$ value corresponding to the $[Ru^{III/II}(edta)(\kappa\ O, \kappa\ O\text{-hpic})]^{3-/4-}$ redox couple, was reported to be 0.0 V (vs. SHE) [46]. It was further noticed that the mixed-chelate complexes of Ru^{II}edta are more stable than the Ru(III) analogue [46].

The bidentate ligand 2-aminomethylpyridine (ampy) coordinates to the Ru(III) center through its pyridine-N and amine group to form the mixed-chelate $[Ru^{III}(edta)(ampy)]^{-}$ complex [47]. The $[Ru^{III}(edta)(ampy)]^{-}$ complex was examined electrochemically

Table 2
Formal potentials ($E_{1/2}$) for the Ru^{III}/Ru^{II} couple in $[Ru^{III}(edta)(L_1\text{-}L_2)]$ (overall charge on the complex is dropped for the sake of convenience).

Bi-dentate ligand (L_1-L_2)	[a] $E_{1/2}$ (V vs. SHE)	Ref.
Picolinate	0.18	[46]
Salicylate	-0.42	[46]
1,10-Phenanthroline	0.65	[51]
2,2′-Bipyridine	0.58	[51]
1,2-bis(Diphenylphosphino)ethane	0.93	[51]
Dopamine	-0.63	[52]
Catecholate	-0.61	[52]

[a] Potentials are converted into SHE where reported with different reference electrodes.

[47] and the formal potential for the $[Ru^{III}(edta)(ampy)]^{-}/[Ru^{II}(edta)(ampy)]^{2-}$ couple measured by cyclic voltammetric studies was found to be at 0.27 V (vs. SHE) at lower pH (4.5) [47]. However, at higher pH, oxidative dehydrogenation of the coordinated 'ampy' ligand takes place, followed by a metal-induced electron transfer process (Scheme 6) to yield the $[Ru^{II}(edta)(impy)]^{2-}$ complex (impy = iminomethylpyridine) [47]. The $E_{1/2}$ value associated with the $[Ru^{III}(edta)(impy)]^{-}/[Ru^{II}(edta)(impy)]^{2-}$ couple was reported to be 0.57 V (vs. SHE) [47].

Toma and co-workers investigated the formation of mixed-chelated complexes of Ru(edta) containing the bi-dentate ligands, *ortho*-phenylenediamine (opda) [48] and 9,10-diaminophenanthrene (pha) [49]. Their studies revealed that both the $[Ru^{III}(edta)(opda)]^{-}$ and $[Ru^{III}(edta)(pha)]^{-}$ mixed-chelated complexes are unstable under aerobic conditions, and undergo oxidative dehydrogenation reactions to yield the corresponding di-imine complexes, $[Ru^{III}(edta)(bqdi)]^{-}$ (bqdi = *ortho*-benzoquinone di-imine) and $[Ru^{III}(edta)(phi)]^{-}$ (phi = 9,10-phenanthrene quinone di-imine), respectively [48,49]. The electrochemistry of these di-imine complexes exhibited metal-centered one-electron (reversible), and two-electron/two proton redox processes as depicted in Scheme 7. The formal potential for the $[Ru^{III/II}(edta)(bqdi)]^{-/2-}$ couple (0.74 V vs. SHE) [48] is higher than that for $[Ru^{III/II}(edta)(phi)]^{-/2-}$ (0.63 V vs. SHE) [49] may be explicable by the fact that the *ortho*-benzoquinone di-imine (bqdi) possesses higher π–acidic character than 9,10-phenanthrene quinone di-imine (phi).

The mixed-chelate $[Ru^{III}(edta)(ddtc)]^{2-}$ (ddtc$^-$ = diethyldithio carbamate) complex was examined by cyclic voltammetry, and the pair of waves observed at $E_{1/2}$ = −0.22 V (vs. SHE) was ascribed to the $[Ru^{III}(edta)(ddtc)]^{2-}/[Ru^{II}(edta)(ddtc)]^{3-}$ redox couple [50]. Spectro-electrochemical studies confirmed that the $[Ru^{II}(edta)(ddtc)]^{3-}$ complex exhibits a band at 434 nm assigned to metal to ligand charge transition ($d\pi \rightarrow \pi^*$) [50].

One general observation noted from the above referred studies is that the formation of the mixed-chelate complexes of Ru(edta) was initiated through the aqua-substitution of the $[Ru^{III}(edta)(H_2O)]^-$ complex resulting in the formation of a mono-substituted mixed-ligand species, followed by the chelation step involving the removal of one coordinated carboxylate arm of the 'edta' ligand to yield the mixed-chelate complexes. The formal potentials ($E_{1/2}$) values associated with the Ru^{III}/Ru^{II} redox couple reported for a few other mixed-chelate complexes of Ru(edta), are listed in Table 2.

3. Electrochemistry of binuclear complexes of Ru(edta)

In 1966, Ezerskaya et al. [53,54] reported that $[Ru^{III}(edta)(H_2O)]^-$ reacts with H_2O_2 to produce a green complex which might be a μ-oxo or μ-peroxo doubly-bridged binuclear complex of Ru (edta), but no evidence was provided in support of the formation of such binuclear species. Later, Shimizu and co-workers [22] reported that the oxidation of $[Ru^{III}(edta)(H_2O)]^-$ with chlorite ion also yielded a green complex, which was characterized as an oxo-bridged mixed-valence binuclear $[(edta)Ru^{IV}\text{-}O\text{-}Ru^{III}(edta)]^{3-}$ complex by spectral and electrochemical studies. It was further reported that the Ru(IV)-Ru(III) dimer could be reduced at the mercury electrode to the Ru(III)-Ru(III) species, which subsequently decomposed to the Ru(III)-monomer complex [22]. Baar and Anson [28] showed that the electrochemical oxidation of $[Ru^{III}(edta)(H_2O)]^-$ progressed in two consecutive half- and one-electron steps producing the $[(edta)Ru]_2(III_{1/2},III_{1/2})$ species (instead of $[(edta)Ru^{IV}\text{-}O\text{-}Ru^{III}(edta)]^{3-}$ reported by Shimizu and co-workers [22]), and the $[(edta)Ru]_2$(IV,IV) dimers are plausibly linked by oxo or dihydroxo bridging ligands [28]. It was further reported that the $[(edta)Ru]_2$(IV,IV) dimer complex exhibited catalytic ability to oxidize water to dioxygen [28]. While examining the catalytic ability of the $[(edta)Ru]_2$(IV,IV) dimer complex, Hurst and co-workers thoroughly reinvestigated the electrochemical properties of the mononuclear $[Ru^{III}(edta)(H_2O)]^-$ and the dinuclear $[(edta)Ru^{III}\text{-}O\text{-}Ru^{IV}(edta)]^{3-}$ complexes [55].

Based on the results of Resonance Raman studies [55] it was unambiguously established that in both $[(edta)Ru^{III}\text{-}O\text{-}Ru^{IV}(edta)]^{3-}$ and $[(edta)Ru^{IV}\text{-}O\text{-}Ru^{IV}(edta)]^{2-}$ complexes, the Ru (edta) units are only linked through a μ-oxo ion. It was further observed that the $[(edta)Ru^{IV}\text{-}O\text{-}Ru^{IV}(edta)]^{2-}$ complex was incapable of catalyzing water oxidation [55] which is not in accord with the observations of Baar and Anson [28]. The electrochemical oxidation of $[(edta)Ru^{III}\text{-}O\text{-}Ru^{IV}(edta)]^{3-}$ yielded $[(edta)Ru^{IV}\text{-}O\text{-}Ru^{IV}(edta)]^{2-}$ species which was found to be unstable under all conditions, and reverted into $[(edta)Ru^{III}\text{-}O\text{-}Ru^{IV}(edta)]^{3-}$ species over a period of time with concomitant evolution of CO_2 gas (which resulted from oxidation of the 'edta' ligand) [55]. The overall electrochemical observations available in the literature [22,28,53–55] regarding the oxo-bridged binuclear complexes of Ru(edta), can be accounted for in terms of Scheme 8.

A group of binuclear complexes of Ru(edta) bridged in another way than through the μ–oxo ion, were first reported by Haim and co-workers [56] who studied the intra-molecular electron transfer reaction in the $[(edta)Ru^{II}\text{-}(BL)\text{-}Co^{III}(NH_3)_5]^+$ binuclear complexes linked with bridging ligands (BL) typically shown in Fig. 8.

Cyclic voltammetric studies of all the $[(edta)Ru^{III}\text{-}(BL)\text{-}Co^{III}(NH_3)_5]^{2+}$ complexes performed, and the $E_{1/2}$ values for the $[(edta)Ru^{III}\text{-}(BL)\text{-}Co^{III}(NH_3)_5]^{2+}/[(edta)Ru^{II}\text{-}(BL)\text{-}Co^{III}(NH_3)_5]^+$ redox couple along with the rate data (k_{et}) for metal-to-metal electron transfer, are tabulated in Table 3. The $E_{1/2}$ values reported for the $Ru^{III/II}$ couples in $[Ru^{III}(edta)(BL)]^-$ are 0.24, 0.15, 0.13, 0.13 and 0.14 V (vs. SHE) for BL = pyrazine, 4,4′-bipyridine, 3,3′-dimethyl-4,4′-'-bipyridine, *trans*-1,2-bis(4-pyridyl)ethylene and 1,4-bis(4-pyridyl)butadiyne, respectively [56]. Considering that the $E_{1/2}$ values of the $Ru^{III/II}$ couple in the $[(edta)Ru^{III}\text{-}(BL)\text{-}Co^{III}(NH_3)_5]^{2+}$ binuclear complexes are not shifted appreciably as compared to their respective mononuclear fragments, the change in the rate constant (k_{et}) values for the electron transfer (Table 3) from the Ru(II)-center to the Co(III)-center via the mentioned bridging ligands (BL), is explicable in terms of the solvent reorganization energy which increases with increasing length of the bridging ligands [56].

Another set of homo-binuclear complexes of the type $[(Hedta)Ru^{III}\text{-}(BL)\text{-}Ru^{III}(Hedta)]$, was synthesized and their electrochemical properties were reported later [57]. Cyclic voltammograms of the $[(Hedta)Ru^{III}\text{-}(BL)\text{-}Ru^{III}(Hedta)]$ binuclear complexes revealed two pairs of cathodic (E_{pc}) and anodic peaks (E_{pa}) with peak to peak separation ($\Delta E_p = E_{pc} - E_{pa}$) values in the range $0.12 < \Delta E < 0.14$ V, indicative of quasi-reversible redox reaction [57]. These peaks were assigned to one-electron transfer redox reactions at each metal center [57] and the formal potentials for the $Ru^{III}\text{-}Ru^{III}/Ru^{III}\text{-}Ru^{II}$ and $Ru^{III}\text{-}Ru^{II}/Ru^{II}\text{-}Ru^{II}$ redox couples, are summarized in Table 4.

Considering that the $E_{1/2}$ value for the $Ru^{III/II}$ redox couple in the mononuclear pyrazine complex of Ru(edta) is 0.24 V (vs. SHE) [18] an anodic shift in the $E^1_{1/2}$ value for the $Ru^{III}\text{-}Ru^{III}/Ru^{III}\text{-}Ru^{II}$ couple and a cathodic shift in the $E^2_{1/2}$ value corresponding to the $Ru^{III}\text{-}Ru^{II}/Ru^{II}\text{-}Ru^{II}$ couple, were observed for the pyrazine bridged symmetrical homo-binuclear Ru(edta) complex as shown in Fig. 9. The observed shift in $E_{1/2}$ values as compared to that of its mononuclear unit, could be explicable with regard to the donor–acceptor type of interaction between the two metal centers of the homo-binuclear

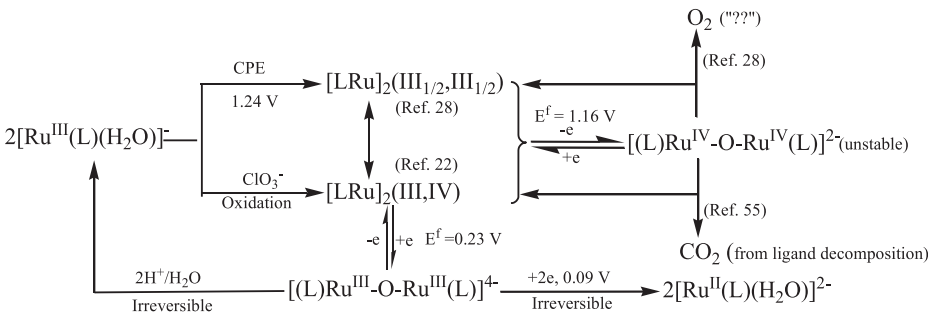

Scheme 8. Electrochemical properties of μ–oxo bridged binuclear complexes of Ru(L), L = edta^{4-}. Potentials are expressed as SHE after standard correction. E^f depicts the formal potential. Reproduced from Ref. [28]

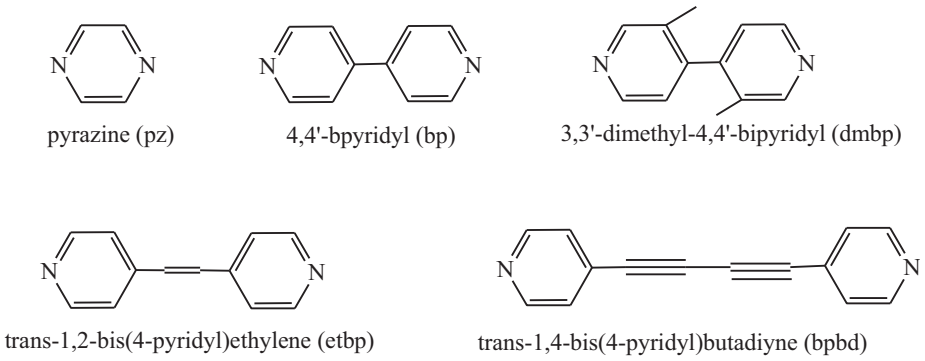

Fig. 8. Schematic presentation of the bridging ligands (BL).

Table 3
$E_{1/2}$ values for Ru^{III}-Co^{III}/Ru^{II}-Co^{III} redox couples and rate constants for intramolecular electron transfer in $[(edta)Ru^{II}$-(BL)-$Co^{III}(NH_3)_5]^{2+}$ binuclear complexes.

Bridging ligands (BL)	[a]$E_{1/2}$ (V vs. SHE)	Metal to metal distance (A°)	k_{et}, s^{-1}
	Not reported	6.8	22.7
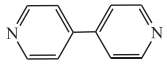	0.13	11.0	0.64
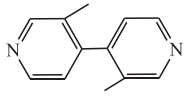	0.12	11.5	0.07
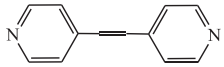	0.11	13.5	0.21
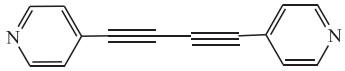	0.15	16.1	0.04

[a] Potentials are converted into SHE where reported with different reference electrodes.

Table 4
$E_{1/2}$ values for Ru^{III}-Ru^{III}/Ru^{III}-Ru^{II} and Ru^{III}-Ru^{II}/Ru^{II}-Ru^{II} redox couples in [(Hedta)Ru^{III}-BL-Ru^{III}(Hedta)] binuclear complexes.

Bridging ligand (BL)	[a]$E^1_{1/2}$ (V vs. SHE)	[a]$E^2_{1/2}$ (V vs. SHE)	$\Delta E_{1/2} = E^1_{1/2} - E^2_{1/2}$ (V vs. SHE)
	0.28	−0.06	0.34
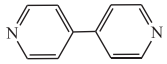	0.17	−0.06	0.23
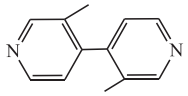	0.16	−0.02	0.18
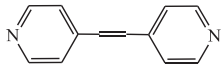	0.17	0.02	0.15

[a] Potentials are converted into SHE where reported with different reference electrodes.

complex (Fig. 9). One of the ruthenium centers in the binuclear complex behaves as a donor exhibiting an anodic shift in the corresponding $E_{1/2}$ value, whereas the cathodic shift in the $E_{1/2}$ value caused by the other ruthenium center acting as an acceptor [57].

In other bipyridyl bridged binuclear complexes of Ru(edta), the cathodic and the anodic shift in the $E_{1/2}$ values were also observed (Table 4) when compared to that of the $Ru^{III/II}$ redox couple of the monomeric $[Ru^{III}(edta)(BL)]^-$ [57] i.e. the monomeric fragment of

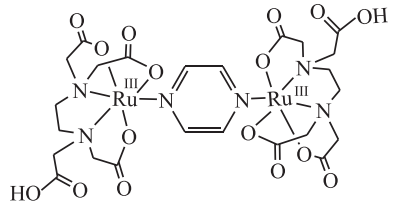

Fig. 9. Schematic presentation of the pyrazine bridged binuclear complex of Ru^{III}(edta).

the aforementioned binuclear complexes. The magnitude of interaction amongst the metal centers in [(Hedta)Ru^{III}-(BL)-Ru^{III}(Hedta)] binuclear complexes estimated by $\Delta E_{1/2}$ value (Table 4), depends on the dimension of the bridging ligands. The larger the size of the bridging ligand, the lower the $\Delta E_{1/2}$ value [57]. Moreover, planarity of the bridging ligand was also reported to play a role to govern the interaction between two metal centers. The bridging ligand 3,3-dimethyl-4,4′-bipyridyl is less planer than 4,4′-bipyridyl, for which the magnitude of interaction ($\Delta E_{1/2}$) between two metal centers is less as compared to that observed (Table 4) in the binuclear complex of Ru(edta) bridged by 4,4′-bipyridyl [57].

Cyclic voltammetric studies of another set of hetero-binuclear $[(Hedta)Ru^{III}$-(BL)-$Fe^{II}(CN)_5]^{3-}$ complexes containing the aforementioned bridging ligands (Fig. 8) conformed the participation of both the Ru and Fe centers in an one-electron redox process [58]. Cyclic voltammograms of such complexes were characterized by two pairs of cathodic and anodic waves, which were assigned to the metal based redox processes. The redox wave for the Ru center was found to be quasi-reversible ($\Delta E_p \sim 0.140$ V). While the $E_{1/2}$ values corresponding to the $Ru^{III/II}$ couple in such hetero-binuclear complexes were reported to be in the range 0.33–0.40 V (vs. SHE), the values for the $Fe^{III/II}$ redox couple, varied between 0.66 and 0.79 V [58]. Based on the small shift observed in the $E_{1/2}$ values of the individual components in the $[(Hedta)Ru^{III}$-

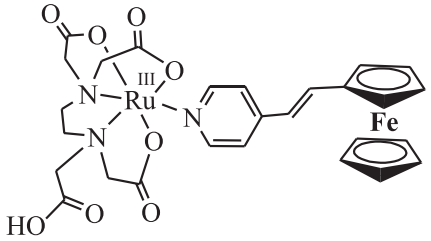

Fig. 10. Schematic presentation of the binuclear complex of Ru^{III}(edta) bridged by *trans*-1-(4-pyridyl)-ethylene)ferrocene. Reproduced from Ref. [60].

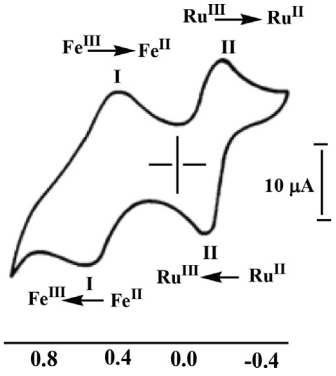

Fig. 11. Cyclic voltammogram of the $[(edta)Ru^{III}\text{-}NC\text{-}Fe^{II}(CN)_5]^{5-}$ complex in aqueous KCl (0.1 M). Adapted with the permission from Inorganic Chemistry, 1993, 32, 4049-4052 Copyright 1993 American Chemical Society.

$(BL)\text{-}Fe^{II}(CN)_5]^{3-}$ complexes, as compared to the $E_{1/2}$ values of their mononuclear $[(Hedta)Ru^{III}\text{-}(BL)]$ and $[Fe(CN)_5\text{-}(BL)]^{3-}$ complexes, it was inferred that the metal–metal interaction in the $[(Hedta)Ru^{III}\text{-}(BL)\text{-}Fe^{II}(CN)_5]^{3-}$ complexes is weak [58]. Interestingly, all the hetero-binuclear $[(Hedta)Ru^{III}\text{-}(BL)\text{-}Fe^{II}(CN)_5]^{3-}$ complexes exhibited intense inter valence charge transfer (IVCT) bands in the near IR region [58].

The $[(Hedta)Ru^{III}\text{-}(BL)\text{-}\beta\text{-}CD\text{-}Fe^{II}(CN)_5]^{3-}$ binuclear complexes, containing the bridging ligands (BL = 1,2-bis(4-pyridyl)ethane and 1,3-bis(4-pyridyl)propane) incorporated into the cavity of the β-cyclodextrine (β-CD), were examined electrochemically and the results of the investigations revealed that the incorporation of the bridging ligands into the cavity of β-cyclodextrine did not improve the metal to metal interaction appreciably as evidenced by the electrochemical studies [59]. The small decrease in $\Delta E_{1/2}$ ($E_{1/2}Ru^{III/II}$ – $E_{1/2}Fe^{III/II}$) of 0.015 V observed while the bridging ligand is caged in the cavity of the β-cyclodextrine, further implies that the inclusion of the bridging ligand in the cavity of the β-cyclodextrine does not alter the potential energy barrier for the electron transfer process.

A report on the use of the ferrocenyl ligand, *trans*-1-(4-pyridyl)-ethylene)ferrocene, towards preparation of a hetero-binuclear complex of Ru(edta), is available in the literature [60]. The binuclear complex (Fig. 10) was subjected to cyclic voltammetric studies and two distinct one-electron redox reactions at the electrode were observed [60]. The $E_{1/2}$ values for the Fe^{II}/Fe^{III} (Fc/Fc^+, Fc – ferrocene) and $Ru^{III/II}$ redox couples estimated from cyclic voltammetric studies are 0.76 V and 0.06 V (vs. SHE), respectively [60]. Considering the anodic shift in $E_{1/2}$ value by 0.080 V for the Fe^{II}/Fe^{III} (Fc/Fc^+) couple and cathodic shift of 0.030 V for the $Ru^{III/II}$ couple, in comparison to their mononuclear counterpart, a donor–acceptor type interaction was proposed for the above mentioned binuclear complex (Fig. 10) [60].

Reports on the spectral and electrochemical studies of cyano-bridged complexes of the type $[(edta)Ru^{III}\text{-}NC\text{-}M^{II}(CN)_5]^{5-}$ (M = Fe, Ru and Os) displaying thermochromism of the IVCT band are available in the literature [61–63]. The electrochemical behavior of the complex was found to be quite intriguing, especially the effect of temperature on the formal potential of the individual metal centers in the above mentioned cyano-bridged binuclear complex [61]. The cyclic voltammogram (Fig. 11) of the $[(edta)Ru^{III}\text{-}NC\text{-}Fe^{II}(CN)_5]^{5-}$ complex displayed more than one reversible peaks (marked as I and II). The peaks were assigned to one-electron transfer redox processes at the Fe and Ru centers, and the $E_{1/2}$ values associated with the $Fe^{III/II}$ and $Ru^{III/II}$ redox couples are 0.69 and 0.02 V (vs. SHE), respectively [61].

The $E_{1/2}$ values associated with the $[(edta)Ru^{III}\text{-}NC\text{-}M^{III}(CN)_5]^{4-}$/ $[(edta)Ru^{III}\text{-}NC\text{-}M^{II}(CN)_5]^{5-}$ and $[(edta)Ru^{III}\text{-}NC\text{-}M^{II}(CN)_5]^{5-}$/$[(edta)Ru^{II}\text{-}NC\text{-}M^{II}(CN)_5]^{6-}$ redox couples are summarized along with the inter valence absorption maxima in Table 5. The anodic shift in the potential pertinent to the $Ru^{III}\text{-}M^{III}/Ru^{III}\text{-}M^{II}$ couples in the mentioned binuclear complexes as compared to the $M^{III/II}$ couples of their $M(CN)_6$ component, independently is expected owing to the existence of the electron-retreating Ru(edta) moiety. However, $E_{1/2}$ values for $Ru^{III}\text{-}M^{II}/Ru^{II}\text{-}M^{II}$ couples (Table 5) in the above referred binuclear complexes are not altered significantly with respect to the formal potential (−0.01 V vs. SHE) reported for the $[Ru^{III/II}(edta)(H_2O)]^{-/2-}$ couple, indicating an insignificant effect of the metal-cyanide moiety on the Ru-center under the chelating environment of the edta ligand.

The $[(edta)Ru^{III}\text{-}NC\text{-}M^{II}(CN)_5]^{5-}$ binuclear complexes exhibited inter valence absorption maxima in the near IR range which is shifted towards higher energy (Table 5) with increasing $E_{1/2}$ values for the $Ru^{III}\text{-}M^{III}/Ru^{III}\text{-}M^{II}$ couples.

The temperature dependence of the inter valence absorption maxima (E_{op}) of the $[(edta)Ru^{III}\text{-}NC\text{-}Fe^{II}(CN)_5]^{5-}$ complex was studied spectrophotometrically and the dE_{op}/dT value was found to be $-5\ cm^{-1}\ deg^{-1}$ [61]. While simplifying the Hush treatment [64] of inter-valence energies (E_{op}), Hupp and Dong [65] reported that E_{op} could be correlated with ΔE (where ΔE is the difference in the formal potential of two redox-responsive metal centers in the binuclear complex) [65]. The effect of temperature on the formal potential (E^f) for the reduction of $[(edta)Ru^{III}\text{-}NC\text{-}Fe^{III}(CN)_5]^{4-}$ to $[(edta)Ru^{III}\text{-}NC\text{-}Fe^{II}(CN)_5]^{5-}$, and the reduction of $[(edta)Ru^{III}\text{-}NC\text{-}Fe^{II}(CN)_5]^{5-}$ to $[(edta)Ru^{II}\text{-}NC\text{-}Fe^{II}(CN)_5]^{6-}$, were studied by cyclic voltammetry. It was noticed that E^f for the Fe center changes appreciably with changes in temperature, but for the Ru center no significant temperature effect on E^f was observed [61]. The value of the temperature-dependence term (dE^f/dT) determined from cyclic voltammetric studies performed at variable temperature, is $-6\ cm^{-1}\ deg^{-1}$, which is in good agreement with the value ($-5\ cm^{-1}\ deg^{-1}$) obtained from the spectral studies [61]. The dE_{op}/dT value for the mixed-valence cyano-bridged homo-binuclear $[(Hedta)Ru^{III}\text{-}NC\text{-}Ru^{II}(CN)_5]^{4-}$ complex determined spectrophotometrically ($-4.1\ cm^{-1}\ deg^{-1}$) was found to be comparable to the value of dE^f/dT ($-3.45\ cm^{-1}\ deg^{-1}$) obtained from variable temperature cyclic voltammetric studies [63].

Spectroscopic and electrochemical properties of $[(edta)Ru^{III}\text{-}NC\text{-}M(CN)_x]^{5-}$ and its isomer, $[(edta)Ru^{III}\text{-}CN\text{-}M(CN)_x]^{5-}$ (M = Fe^{II}, x = 5; M = Mo^{IV}, x = 7) determined by spectral and electrochemical studies at varied temperature and pressure, were reported by van Eldik and co-workers [66]. While an increase in $E_{1/2}$ value (0.11 V

Table 5
Formal potentials for $Ru^{III}\text{-}M^{III}/Ru^{III}\text{-}M^{II}$ and $Ru^{III}\text{-}M^{II}/Ru^{II}\text{-}M^{II}$ redox couples and IVCT bands of the in $[(edta)Ru^{III}\text{-}NC\text{-}M^{II}(CN)_5]^{5-}$ complexes measured in aqueous solution at pH 5.5.[a)]

M	$E^1_{1/2}$ for $Ru^{III}\text{-}M^{III}/Ru^{III}\text{-}M^{II}$ (V vs. SHE)	$E^2_{1/2}$ for $Ru^{III}\text{-}M^{III}/Ru^{III}\text{-}M^{II}$ (V vs. SHE)	$\Delta E_{1/2} = E^1_{1/2} - E^2_{1/2}$ (V vs. SHE)	Inter valence absorption maxima (nm)
Fe	0.43	−0.08	0.51	940
Os	0.67	−0.01	0.68	762
Ru	0.97	0.00	0.97	674

[a)] Potentials are converted into SHE where reported with different reference electrodes.

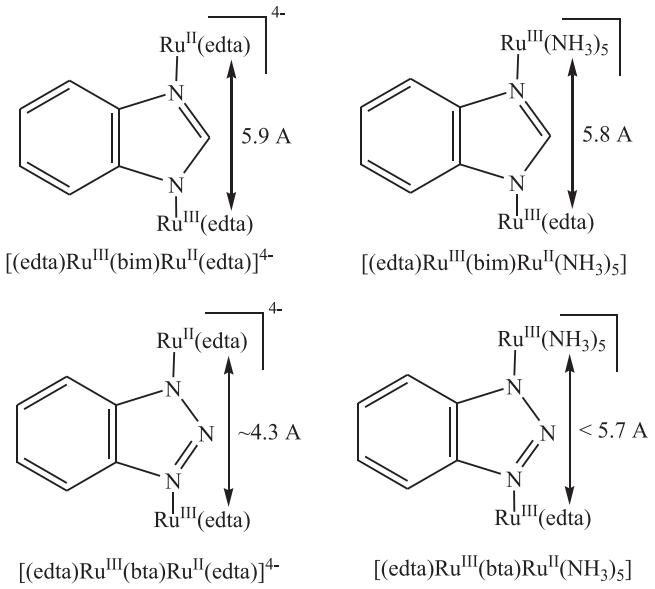

Fig. 12. Schematic presentation of the benzimidazolate and benzotriazolate bridged binuclear complexes of Ru^{III}(edta). Reproduced from Ref. [70].

vs. SHE) by 0.085 V for the Ru^{III}-Fe^{II}/Ru^{II}-Fe^{II} couple in $[(edta)Ru^{III}\text{-}CN\text{-}Fe^{II}(CN)_5]^{5-}$ was noticed in comparison to that observed in the $[(edta)Ru^{III}\text{-}NC\text{-}Fe^{II}(CN)_5]^{5-}$ isomer [61], a less positive shift by 0.07 V of the $E_{1/2}$ value (0.415 V vs. SHE) for the Ru^{III}-Fe^{III}/Ru^{III}-Fe^{II} couple for $[(edta)Ru^{III}\text{-}CN\text{-}Fe^{II}(CN)_5]^{5-}$ was observed than that reported ($E_{1/2}$ = 0.485 V vs. SHE) for the $[(edta)Ru^{III}\text{-}NC\text{-}Fe^{II}(CN)_5]^{5-}$ isomer [61]. An identical trend was observed for the $[(edta)Ru^{III}(NC)Mo^{IV}(CN)_7]^{5-}$ and $[(edta)Ru^{III}(CN)Mo^{IV}(CN)_7]^{5-}$ isomers [66]. This group further studied the effect of hydrostatic pressure on the $Ru^{III/II}$ and $Fe^{III/II}$ redox couples in two binuclear complexes, $[(edta)Ru^{III}\text{-}NC\text{-}Fe^{II}(CN)_5]^{5-}$ and $[(NH_3)_5Ru^{III}\text{-}NC\text{-}Fe^{II}(CN)_5]^{-}$ [67] and the results of the high-pressure cyclic voltammetric studies revealed that the change in volume ($\Delta V_{complex}$) because of reduction of the Fe center in both cases was unaffected by the charge type on the Ru center (from +3 to −1) in the binuclear complexes [67].

In the recent past, electrochemical properties of $[(edta)Ru^{III}\text{-}NC\text{-}Fe^{II}(CN)_5]^{5-}$ attached to the surface of silica gel that was chemically modified with zirconium(IV) oxide (hereafter designated as ΞZrFeRu) were reported by Lazarin and co-workers [68]. Cyclic voltammetric measurements were performed on a modified carbon paste working electrode prepared by mixing graphite and ΞZrFeRu. Two pairs of reversible peaks were found which were assigned to the $Ru^{III/II}$ ($E_{1/2}$ = −0.04 V vs. SHE) and $Fe^{III/II}$ ($E_{1/2}$ = 0.14 V vs. SHE) redox couples [68]. A negative shift of the $E_{1/2}$ values with respect to that reported for the free $[(edta)Ru^{III}\text{-}NC\text{-}Fe^{II}(CN)_5]^{5-}$ complex in solution [51] was observed for which the absorption maximum of the IVCT band was positioned in the higher energy range (800 nm) [68]. The observed negative shift of the $E_{1/2}$ values as compared to that of the free $[(edta)Ru^{III}\text{-}NC\text{-}Fe^{II}(CN)_5]^{5-}$ complex in solution [61] was attributed to the interaction between ΞZrFeRu with an excess of $[Fe^{II}(CN)_6]^{4-}$ immobilized on the surface of the zirconium oxide modified silica gel [68].

The use of benzimidazolate (bim) and benzotriazolate (bta) as bridging ligands towards preparation of both symmetric and asymmetric homo-binuclear complexes of Ru(edta), was explored by Toma and co-workers [69,70].

All the binuclear complexes shown in Fig. 12, were examined cyclic voltammetrically and spectro-electrochemically, and based on the results (Table 6) and considering the $E_{1/2}$ values reported for the mononuclear fragments of the asymmetric binuclear bridged complexes [60], one-electron redox reactions at the electrode are outlined (Eqs. (11a) and (11b)) in Scheme 9.

Use of 4-sulfanylpyridine as bridging ligand for preparing the binuclear complexes of Ru(edta) (Fig. 13) was reported by van Eldik and coworkers [71]. Cyclic voltammetry of the bridged Ru(edta) complex shown in Fig. 13 exhibited two pairs of cathode and anodic peaks at pH < 3, and the estimated values of the formal potentials at 0.33 and −0.10 V (vs. SHE) were attributed to $[(Hedta)Ru^{III}\text{-}N\Xi S\text{-}Ru^{III}(Hedta)]/[(Hedta)Ru^{II}\text{-}N\Xi S\text{-}Ru^{III}(Hedta)]^{-}$ and $[(Hedta)Ru^{II}\text{-}N\Xi S\text{-}Ru^{III}(Hedta)]^{-}/[(Hedta)Ru^{II}\text{-}N\Xi S\text{-}Ru^{II}(Hedta)]^{2-}$ redox couples, respectively [71]. However, a cathodic shift of 0.280 V observed for the $[(edta)Ru^{II}\text{-}N\Xi S\text{-}Ru^{III}(edta)]^{4-}/[(edta)Ru^{II}\text{-}N\Xi S\text{-}Ru^{II}(edta)]^{5-}$ redox couple at higher pH (~8) is plausibly associated with the change in coordination mode of the bridging ligand, from thione (at pH < 3) to thiol (at pH ~ 8) as shown in Fig. 13.

4. Electro-catalysis with Ru^{III}(edta) complexes

Electrochemical properties of Ru(edta) complexes discussed in the above sections, not only provide insight into the redox-active nature of the Ru(edta) complexes, but clearly signify their ability to operate as potential 'molecular catalysts' for electrochemical transformation in homogeneous solution involving an electrode as a heterogeneous outer-sphere electron donor or acceptor. Moreover, $[Ru^{III}(edta)(H_2O)]^{-}$ due to its intrinsic lability, could easily bind to substrate molecules (via rapid substitution reactions), thus providing a lower energy pathway (rendering substantial drop in over-potential required to initiate the electrochemical conversion of substrate directly) for the redox transformation of the substrate via multi-electron transfer processes.

4.1. Electro-catalytic reduction of nitrite using the $[Ru^{III}(edta)(H_2O)]^{-}$ complex

Though enzymatic (nitrite reductase) reduction of nitrite is a complicated multi-electron process [72], Meyer et al. [73,74] reported that the $[Ru(edta)(H_2O)]^{-}$ complex could affect the electrochemical reduction of nitrite (NO_2^-) to various N-based products (N_2O, N_2, NH_2OH and NH_3). The process was examined by performing exhaustive controlled potential electrolysis (using a mercury pool as working electrode) at different pH and applied potentials under turnover conditions of excess nitrite [74]. The relative amount of each product in the mixture of products (N_2O, N_2, NH_2OH and NH_3) formed in the reduction of nitrite, depended on the

Table 6
$E_{1/2}$ values for Ru^{III}-Ru^{III}/Ru^{III}-Ru^{II} and Ru^{III}-Ru^{II}/Ru^{II}-Ru^{II} redox couples, and inter valence absorption maxima (E_{op}) reported for benzotriazolate (bim) and benzimidazolate (bta) binuclear complexes of Ru(edta).

Binuclear complex	[a] $E^1_{1/2}$ (V vs. SHE)	[a] $E^2_{1/2}$ (V vs. SHE)	$\Delta E_{1/2} = E^1_{1/2} - E^2_{1/2}$ (V vs. SHE)	E_{op} (nm)
$[(edta)Ru^{III}(bim)Ru^{II}(edta)]^{4-}$	−0.09	−0.23	0.14	1500 (broad)
$[(edta)Ru^{III}(bta)Ru^{II}(edta)]^{4-}$	0.02	−0.18	0.20	1450
$[(edta)Ru^{III}(bim)Ru^{II}(NH_3)_5]$	0.035	−0.175	0.21	1450
$[(edta)Ru^{III}(bta)Ru^{II}(NH_3)_5]$	0.175	−0.110	0.285	1500 (broad)

[a] Potentials are converted into SHE where reported with different reference electrodes.

$$E^1_{1/2} = 0.035\ V \qquad E^2_{1/2} = -0.175\ V$$
$$[(edta)Ru^{III}(bim)Ru^{III}(NH_3)_5]^{+} \overset{+e}{\underset{-e}{\rightleftharpoons}} [(edta)Ru^{III}(bim)Ru^{II}(NH_3)_5]^{0} \overset{+e}{\underset{-e}{\rightleftharpoons}} [(edta)Ru^{II}(bim)Ru^{II}(NH_3)_5]^{-} \quad (11a)$$

$$E^1_{1/2} = 0.175\ V \qquad E^2_{1/2} = -0.110\ V$$
$$[(edta)Ru^{III}(bta)Ru^{III}(NH_3)_5]^{+} \overset{+e}{\underset{-e}{\rightleftharpoons}} [(edta)Ru^{III}(bta)Ru^{II}(NH_3)_5]^{0} \overset{+e}{\underset{-e}{\rightleftharpoons}} [(edta)Ru^{II}(bta)Ru^{II}(NH_3)_5]^{-} \quad (11b)$$

Scheme 9. Schematic presentation of the electrochemical redox reactions of benzotriazolate (bim) and benzimidazolate (bta) bridged asymmetric binuclear complexes of Ru (edta).

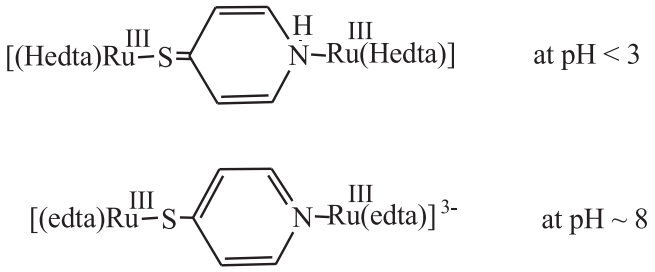

Fig. 13. Schematic presentation of the 4-sulfanylpyridine (NΞS) bridged binuclear complexes of Ru^{III}(edta).

applied potential and pH of the reaction system [74]. It was shown that under turnover conditions, 97% of the total nitrite could be reduced at pH 2.1 (at −0.31 V vs. SHE), whereas, 86% conversion was noticed at pH 5.0 9 (at −0.51 V vs. SHE) [74]. Further increase in pH decreased the catalytic efficiency of the system due to oxidative degradation of the catalyst complexes at higher pH [74]. The nitrosyl complex, $[Ru^{II}(edta)(NO^+)]^-$, was proposed to be the key species responsible for the effective catalytic process, and the formation of $[Ru^{II}(edta)(NO^+)]^-$ in the overall electro-catalytic process is shown in Scheme 10. The $[Ru^{III}(edta)(H_2O)]^-$ complex reacts with NO_2^- to from the $[Ru^{III}(edta)(NO_2)]^{2-}$ complex, which undergoes decomposition (Eq. (12)) at lower pH (<5) yielding $[Ru^{III}(edta)(NO^+)]^0$ species in the reacting system [75]. This $[Ru^{III}(edta)(NO^+)]^0$ complex could further experience metal-centered one-electron reduction to produce $[Ru^{II}(edta)(NO^+)]^-$ [33]. Formation of $[Ru^{II}(edta)(NO^+)]^-$ could also take place in the reaction of $[Ru^{II}(edta)(H_2O)]^{2-}$ with NO_2^- (Eq. (13)) [76].

The $[Ru^{II}(edta)(NO^+)]^-$ species could undergo a further one-electron reduction at −0.11 V (vs. SHE) [30,74] to produce an unstable intermediate species, $[Ru^{II}(edta)(NO\bullet)]^{2-}$ (Eq. (14)) which experienced further reduction (Eqs. (15) and (16)) as noticed in cyclic voltammetric studies [74].

$$\left[Ru^{II}(edta)(NO^+)\right]^- \overset{-0.11V\ vs\ SHE + e}{\underset{-e}{\rightleftharpoons}} \left[Ru^{II}(edta)(NO^\bullet)\right]^{2-} \quad (14)$$

$$\left[Ru^{II}(edta)(NO^\bullet)\right]^{2-} + e \rightarrow [Ru(edta)(NO)]^{3-} \quad (15)$$

$$\left[Ru^{II}(edta)(NO^\bullet)\right]^{2-} + e + H^+ \rightarrow \left[Ru^{II}(edta)(NHO)\right]^{2-} \quad (16)$$

Based on the above observations, a mechanism involving the initial disproportionation of $[Ru^{II}(edta)(NO\bullet)]^{2-}$, followed by N-N coupling to produce N_2O was proposed (Eqs. (17) and (18)) [74].

$$2\left[Ru^{II}(edta)(NO^\bullet)\right]^{2-} + H^+ \rightarrow \left[Ru^{II}(edta)(NO^+)\right]^- + [Ru(edta)(NHO)]^{2-} \quad (17)$$

$$2[Ru(edta)(NHO)]^{2-} + H_2O \rightarrow 2\left[Ru^{II}(edta)(H_2O)\right]^{2-} + N_2O \quad (18)$$

Formation of N_2 was also accounted for by further reduction of $[Ru(edta)(NHO)]^{2-}$ involving N-N coupling [74] as shown in Eq. (19).

$$2[Ru(edta)(NHO)]^{2-} + 2H^+ + 2e \rightarrow 2\left[Ru^{II}(edta)(H_2O)\right]^{2-} + N_2 \quad (19)$$

More highly reduced products, NH_3OH^+ and NH_4^+, were formed via two-electron reduction and formation of NH_2OH [74] as outlined in Eqs. (20)–(22).

$$[Ru(edta)(NHO)]^{2-} + 2H^+ + 2e \rightarrow 2\left[Ru^{II}(edta)(NH_2OH)\right]^{2-} \quad (20)$$

$$\left[Ru^{II}(edta)(NH_2OH)\right]^{2-} + H^+ \rightarrow \left[Ru^{II}(edta)(NH_3OH)\right]^- \quad (21)$$

$$\left[Ru^{II}(edta)(NH_3OH)\right]^- + H^+ + 2e \rightarrow \left[Ru^{II}(edta)(NH_3)\right]^{2-} + H_2O \quad (22)$$

It was reported that NH_3OH^+ appeared to be a precursor for NH_4^+ which is formed as a transient species that prevents binding and further reduction to NH_3/NH_4^+ [74].

4.2. Electro-catalytic reduction of hydrazine using the $[Ru^{III}(Hedta)(H_2O)]$ complex

In 1994, Ramachandraiah reported that the $[Ru^{III}(Hedta)(H_2O)]$ complex could reduce hydrazine to ammonia electrochemically [77]. The electrochemical properties of the hydrazine bound complex of Ru(edta) was assessed by polarographic and cyclic voltammetric studies. Efficacy of the $[Ru^{III}(Hedta)(H_2O)]$ complex towards catalyzing electrochemical reduction of hydrazine was examined by performing controlled potential electrolysis. Bulk electrolysis

$$[Ru^{III}(edta)(H_2O)]^- + NO_2^- \xrightarrow{-H_2O} [Ru^{III}(edta)(NO_2)]^{2-} \xrightarrow{+2H^+} [Ru^{III}(edta)(NO^+)] + H_2O \quad (12)$$
$$-e \downarrow\uparrow +e \qquad\qquad -e \downarrow\uparrow +e$$
$$[Ru^{II}(edta)(H_2O)]^{2-} + NO_2^- \xrightarrow{-H_2O} [Ru^{II}(edta)(NO_2)]^{3-} \xrightarrow{+H_2O} [Ru^{II}(edta)(NO^+)]^- + 2OH^- \quad (13)$$

Scheme 10. Formation of $[Ru^{II}(edta)(NO^+)]^-$ via NO_2^- reduction.

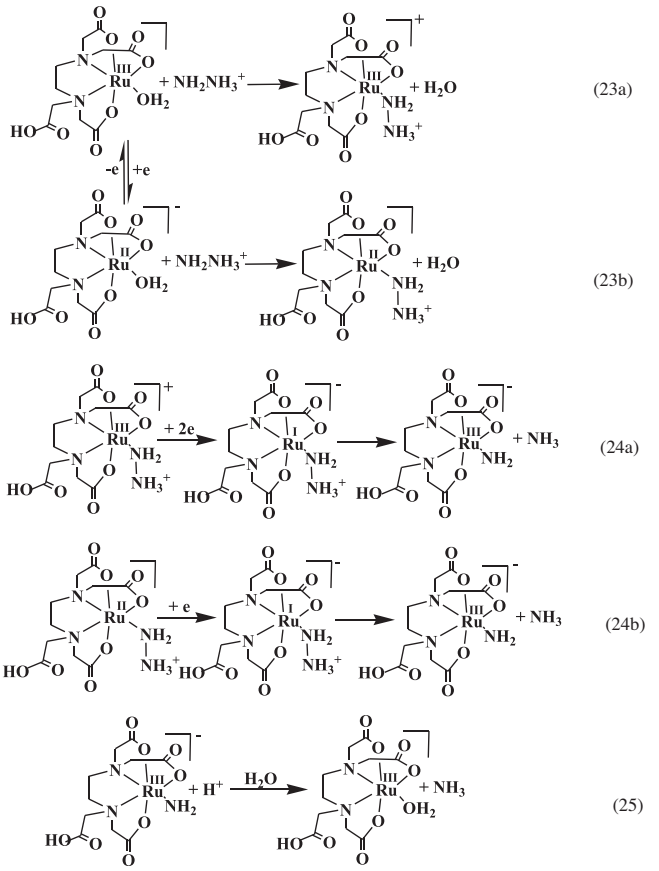

Scheme 11. Electrochemical reduction of hydrazine to ammonia catalyzed by $[Ru^{III}(Hedta)(H_2O)]$ complex. Insert (23a), (23b), (24a), (24b), (25) on the right hand side of the above reactions from top to bottom

of the solution containing the $[Ru^{III}(Hedta)(H_2O)]$ complex and hydrazine (present in large excess) was performed at 0.19 V (vs. SHE) over a mercury pool (as working electrode) for six hours. The catalytic turn-over rate in terms of NH_3 formation (via reduction of hydrazine) was found to be 18.4 and 9.5 ($mol.h^{-1}$) at pH 2.8 and 1.9, respectively, with 100% coulombic efficiency [77].

The overall catalytic process as depicted in Scheme 11 is initiated by the rapid binding of the substrate hydrazine to the catalyst complex via the rapid aqua-substitution step (Eq. (23a)) to produce catalytically active $[Ru^{III}(Hedta)(NH_2NH_3)]^+$ species (Eq. (23a)), which subsequently undergoes a two-electron electrochemical reduction to yield a highly unstable $[Ru^{I}(Hedta)(NH_2NH_3)]^-$ intermediate species (Eq. (24a)) [67]. N-N bond cleavage involving intra-molecular electron transfer in the $[Ru^{I}(Hedta)(NH_2NH_3)]^-$ intermediate, produced $[Ru^{III}(Hedta)(NH_2)]^-$ with concomitant formation of NH_3 (Eq. (24a)) in the reaction system [77]. Hydrolysis of the $[Ru^{III}(edta)(NH_2)]^-$ complex at lower pH (<3) generated another molecule of NH_3 (Eq. (25)) along with the $[Ru^{III}(Hedta)(H_2O)]$ catalyst complex the reaction system [77].

In later studies, Ramachandraiah et al. reported that in presence of the $[Ru^{III}(Hedta)(H_2O)]$ complex, electro-catalytic conversion of phenylhydrazine to ammonia and aniline could be achieved at 0.065 V (vs. SHE) with a turnover rate 5.98 ($mol.h^{-1}$) at pH 2.82 [78]. A catalytic scheme initiated by the formation of $[Ru^{III}(Hedta)(NH_2NHPh)]$ through aqua-substitution of $[Ru^{III}(Hedta)(H_2O)]$ by phenylhydrazine followed by electrochemeical reduction of coordinated phenyhydrazine in $[Ru^{III}(Hedta)(NH_2NHPh)]$ to ammonia and aniline, was proposed [78].

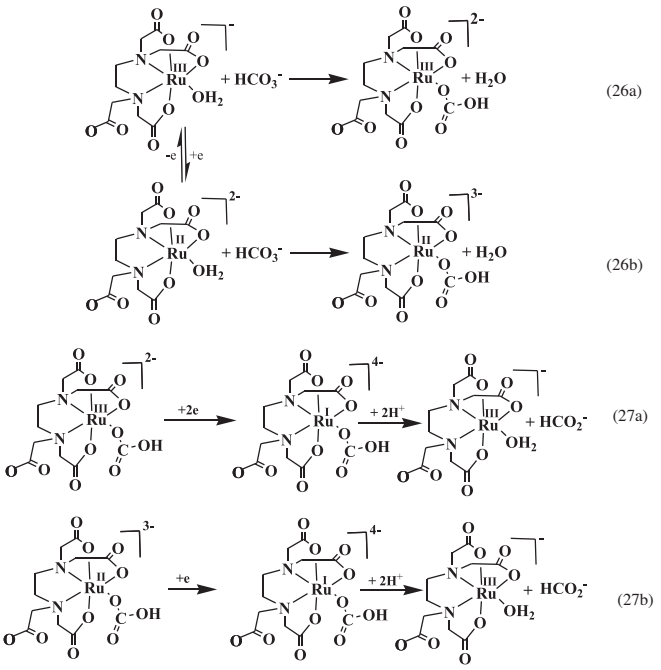

Scheme 12. Electrochemical reduction of bicarbonate to formate catalyzed by $[Ru^{III}(edta)(H_2O)]^-$ complex.

4.3. Electro-catalytic reduction of bicarbonate using the $[Ru^{III}(edta)(H_2O)]^-$ complex

It has been reported that a more negative potential (than −0.36 V vs. SHE [79]) is required for two phase electro-catalytic reduction of gaseous CO_2. It had been reported that the reduction of bicarbonate to formate could be achievable yet at lesser negative potential, −0.16 V vs. SHE, in the aqueous phase by involving $[Ru^{III}(edta)(H_2O)]^-$ as catalyst [80]. The $[Ru^{III}(edta)(H_2O)]^-$ catalyst complex reacts with HCO_3^- to produce $[Ru^{III}(edta)(HCO_3)]^{2-}$. Cyclic voltammetric studies of $[Ru^{III}(edta)(HCO_3)]^{2-}$ showed a reduction wave at −0.16 V (vs. SHE) with a large peak current as compared to the oxidation wave under the turn-over conditions of excess HCO_3^- [80]. These observations imply the occurrence of a catalytic process wherein the $[Ru^{III}(edta)(HCO_3)]^{2-}$ undergoes electrochemical reduction (at −0.16 V vs. SHE) to produce a transient species which was repeatedly produced and spent until the bicarbonate present in the reaction mixture is exhausted [80].

At pH 6.4, bulk electrolysis of a solution containing the $[Ru^{III}(edta)(H_2O)]^-$ catalyst and bicarbonate (present in excess) was carried out at −0.16 V (vs. SHE) over a mercury pool.

Formate was found to be the only detectable product in 67% yield with regard to the initial concentration of bicarbonate under the employed conditions [60]. The catalytic system exhibited 90% Faradic efficiency, and the overall experimental observations are shown in Scheme 12. Under the employed conditions, $[Ru^{III}(edta)(HCO_3)]^{2-}$ and $[Ru^{II}(edta)(HCO_3)]^{3-}$ complexes formed via aqua-substitution reactions (Eqs. (26a) and (26b)) undergo electrochem-

$$O_2 + 4e^- + 4H^+ \rightleftharpoons 2H_2O \qquad E^o = 1.229\ V\ vs\ SHE \quad (28)$$

$$O_2 + 2e^- + 2H^+ \rightleftharpoons H_2O_2 \qquad E^o = 0.695\ V\ vs\ SHE \quad (29)$$

$$H_2O_2 + 2e^- + 2H^+ \rightleftharpoons 2H_2O \qquad E^o = 1.763\ V\ vs\ SHE \quad (30)$$

Scheme 13. Pictorial presentation of proton-coupled electron transfer reactions for dioxygen reduction.

$$[Ru^{III}(edta)(pz)]^{-} + HS^{-} \xrightarrow{k_r} [Ru^{II}(edta)(pz)]^{2-} + HS^{\bullet} \quad (31)$$

$$[Ru^{III}(edta)(pz)]^{-} + HS^{\bullet} \longrightarrow [Ru^{II}(edta)(pz)]^{2-} + S + H^{+} \quad (32)$$

Scheme 14. Pictorial presentation of the reduction of $[Ru^{III}(edta)(pz)]^{-}$ with HS^{-}. Taken from Ref. [82] with permission from the Royal Society of Chemistry.

ical reduction at the applied potential (−0.16 V vs. SHE) producing a transient $[Ru^{I}(edta)(HCO_3)]^{4-}$ intermediate (Eq. (27a) and (27b)) which consequently decomposes involving an inner-sphere proton-coupled electron transfer process to yield HCO_2^- along with the $[Ru^{III}(edta)(H_2O)]^{-}$ catalyst back in the reacting solution (Eqs. (27a) and (27b)) [80].

5. Catalytic implications of Ru^{III}(edta) complexes and challenges

Electrochemical transformation of a substrate molecule in the absence of a catalyst needs a considerable over-potential for advancement of the reaction at an appreciable rate. Owing to its lability to aqua-substitution reactions, the $[Ru^{III}(edta)(H_2O)]^{-}$ complex readily binds to the substrate molecule, and thus lowers the energy barrier of over-potential required for the electrochemical transformation of the small substrate molecules which is archetypically exemplified in the reduction of nitrite ion to ammonia [74] hydrazine to ammonia [77] and bicarbonate to formate [80].

An example of chemical transformations catalyzed by the Ru(edta) complexes in resemblance of metalloenzymes, is discussed in this section related to the reduction of dioxygen (O_2), relevant to the transformation of small molecules. The proton assisted electrochemical reduction of O_2 to H_2O_2 and/or H_2O is shown in Scheme 13 along with the standard potential [81] for the corresponding reaction.

We reported earlier that the $[Ru^{III}(edta)(pz)]^{-}$ (pz = pyrazine) complex could reduce O_2 to H_2O_2 in the presence of H_2S [82]. It is important to note here that the coordinated pyrazine in $[Ru^{III}(edta)(pz)]^{-}$ is not easily exchangeable like the aqua molecule in $[Ru^{III}(edta)(H_2O)]^{-}$ [18]. As discussed in the preceding section, the $E_{1/2}$ value corresponding to the $[Ru^{III}(edta)(pz)]^{-}/[Ru^{II}(edta)(pz)]^{2-}$ redox couple was reported [18] to be 0.24 V (Table 1). As depicted in Scheme 14, the reduction of $[Ru^{III}(edta)(pz)]^{-}$ by HS^{-} takes place involving an outer-sphere pathway (Eq. (31)) leading to the formation of $[Ru^{II}(edta)(pz)]^{2-}$ and the HS**.** radical. In the subsequent step (Eq. (32)) reduction of one more molecule of

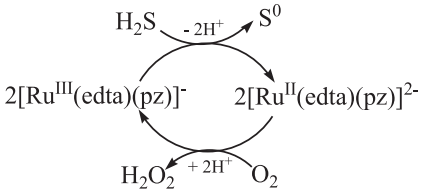

Scheme 15. Pictorial representation of $[Ru^{III}(edta)(pz)]^{-}$ catalyzed reduction of O_2 to H_2O_2. Taken from Ref. [82] with permission from the Royal Society of Chemistry.

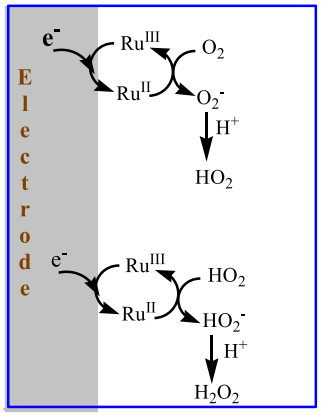

Fig. 15. Electrochemical reduction of O_2 to H_2O_2 catalyzed by $[Ru^{III}(edta)(pz)]^{-}$. Ru^{III} = $[Ru^{III}(edta)(pz)]^{-}$ and Ru^{II} = $[Ru^{II}(edta)(pz)]^{2-}$

$[Ru^{III}(edta)(pz)]^{-}$ by HS**.** to form $[Ru^{II}(edta)(pz)]^{2-}$ and sulfur (S) occurs.

It is worth mentioning here that during oxidation of $[Ru^{II}(edta)(pz)]^{2-}$ by O_2, spectral features of the $[Ru^{II}(edta)(pz)]^{-}$ complex gradually disappeared (Fig. 14a) with concomitant formation of H_2O_2 with 88% yield [82]. The induction period as seen in the time-course of the reaction (Fig. 14b), clearly demonstrates the catalytic nature of the reaction which involved continual regeneration of the Ru(II)-complex in the reacting system after each catalytic cycle. A catalytic cycle resembling the enzymatic activity of oxidoreductases may be constructed (Scheme 15) with the aforementioned reduction of $[Ru^{III}(edta)(pz)]^{-}$ (by HS^{-}) to $[Ru^{II}(edta)(pz)]^{2-}$ and oxidation of $[Ru^{II}(edta)(pz)]^{2-}$ (by O_2) to $[Ru^{III}(edta)(pz)]^{-}$ again [83]. In the overall reactions, dioxygen (O_2) is reduced

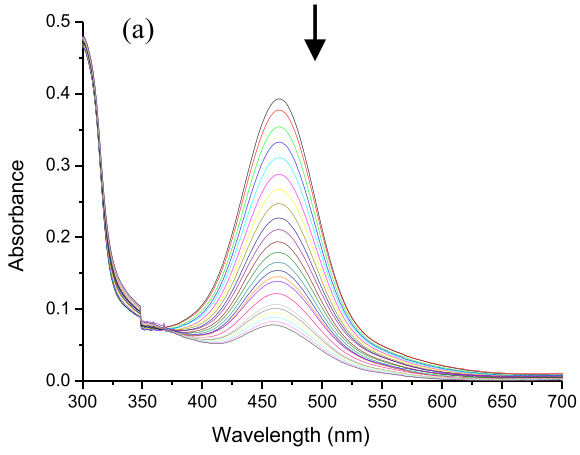

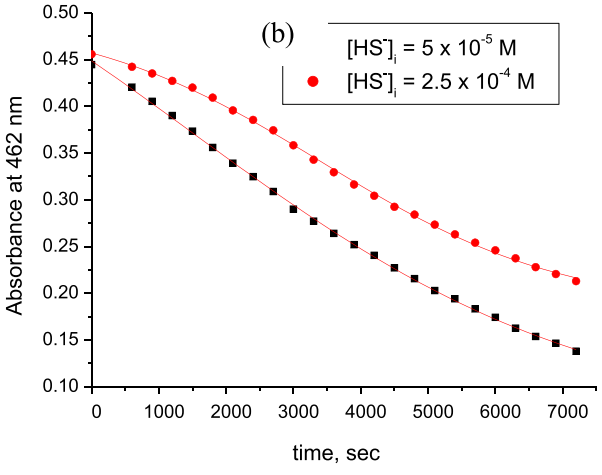

Fig. 14. (a) Decrease in intensity of the metal to ligand charge transfer band of $[Ru^{II}(edta)(pz)]^{2-}$ during the course of its reaction with O_2 and (b) absorption vs. time traces as a function of $[HS^{-}]$. Taken from Ref. [82] with permission from the Royal Society of Chemistry.

to hydrogen peroxide (H_2O_2) via electron transfer reaction, and $[Ru^{III}(edta)(pz)]^-$ complex acts as a redox relay for electron transmission from H_2S to O_2 [82].

The mentioned example of chemical catalysis (Scheme 15) of the reduction of O_2, leads to the idea of using electrons from an electrode (instead of using H_2S) to effect electrochemical reduction of O_2 to H_2O_2 in the presence of $[Ru^{III}(edta)(pz))]^-$ in aqueous acidic solution as demonstrated in Fig. 15. Nevertheless, the $[Ru^{III}(edta)(pz)]^-$ catalyzed electrochemical reduction of O_2 to H_2O_2 as speculatively shown in Fig. 15, whether practically feasible or not, the challenge lies in effecting the reduction of O_2 directly to H_2O. It is important to note here that transfer of four-electrons to O_2 to directly produce water is highly important in the domain of fuel cells and metal-air batteries [84].

Another important aspect is that although the reduction of hydrogen peroxide to water (Eq. (30)) is seemingly easier thermodynamically than the reduction of dioxygen to hydrogen peroxide (Eq. (29)), it is kinetically very difficult as it involves O-O bond breaking. It may be noted that the $[Ru^{V}(edta)(O)]^-$ complex formed in the reaction of $[Ru^{III}(edta)(H_2O)]^-$ with H_2O_2, can react with H_2O_2 (present in excess) to produce O_2 and H_2O in resemblance to catalase activity [85]. Although comprehensive efforts have been made for more than the last two decades, mechanistic details of the direct reduction of O_2 to H_2O resembling *cytochrome c* oxidase [86] are still lacking.

6. Conclusions

The intriguing electrochemical properties of Ru(edta) complexes are brought together and thoroughly evaluated herein for the first time highlighting their catalytic efficiencies in effecting the electrochemical transformations of some small molecules of environmental significance. The results described in this review evidently confirm the observation that a number of mixed-ligand, and mixed-chelate complexes could well participate in electron transfer processes – thus substantiating an important pre-requisite for their redox mediating ability to affect the electron transfer reaction. The wide range of metal-centered redox potentials (Tables 1 and 2) may be of help in understanding the nature of substituted ligands and the design of new catalytic systems to appreciate the potential range required for the particular redox reaction. Electrochemistry of Ru(edta) complexes immobilized on the solid surface of electrodes discussed in this review, signify the scope of heterogenization of homogeneous catalysts which imparts durability to the catalytic system and facilitates the ease to separate the catalyst from catalytic mixtures. The electrochemical properties of binuclear mixed valence complexes of Ru(edta) discussed in this article could be of importance with respect to the development of electrochromic devices [87] apart from providing a significant scope for deeper mechanistic understanding of intra-molecular electron transfer reactions. The ability of $[Ru(edta)(H_2O)]^-$ towards the facile binding of incoming small molecule substrates (viz. NO_2^-, NH_2NH_2, HCO_3^-), and thus lowering their energy barrier for electrochemical transformation, has been categorically established in the case of electrochemical transformations of NO_2^- to NH_3 [74], NH_2NH_2 to NH_3 [77], and HCO_3^- to HCO_2^- [80]. Moreover, the $edta^{4--}$ ligand can exert fine control over both the kinetics and thermodynamics of reactions of catalytic importance.

The prospect of Ru(edta) complexes as redox and/or chemical catalysts for electrochemical transformation of small molecules, concerns of the current decade, are actually established by the aforementioned examples. Although exhaustive research efforts focusing on small molecule activation have been devoted for more than two decades, realization of the catalytic system that mimics enzymatic processes satisfactorily in terms of efficiency and durability, is far from achieved. The electrochemistry of Ru(edta) complexes discussed herein, along with the mechanistic issues, are of relevance, and may provide a basis towards development of more efficient and durable catalyst complexes, and stimulate more intensive research to meet the contemporary energy and environmental challenges related to the small molecule transformations as referred to above.

Declaration of Competing Interest

The authors declare that they have no known competing financial interests or personal relationships that could have appeared to influence the work reported in this paper.

Acknowledgement

DC and RvE thank their co-workers and collaborators who have contributed to this study.

References

[1] G. Qing, R. Ghazfar, S.T. Jackowski, F. Habibzadeh, M.M. Ashtiani, C.-P. Chen, M. R. Smith, T.W. Hamann, Chem. Rev. 120 (2020) 5437.
[2] J.-W. Wang, W.-J. Liu, D.-C. Zhong, T.-B. Lu, Coord. Chem. Rev. 378 (2019) 237.
[3] W. Zhou, X. Meng, J. Gao, A.N. Alshawabkeh, Chemosphere 225 (2019) 588.
[4] M.R. Filipovic, J. Zivanovic, B. Alvarez, R. Banerjee, Chem. Rev. 118 (2018) 1253.
[5] W. Zhang, W. Lai, R. Cao, Chem. Rev. 117 (2017) 3717.
[6] R.J. Crutchley, Coord. Chem. Rev. (Special issue on Molecule Activation) 334 (2017) 1–232.
[7] M. Shao, Q. Chang, J.-P. Dodelet, R. Chenitz, Chem. Rev. 116 (2016) 3594.
[8] B. Milani, G. Licini, E. Clot, M. Albrecht, Dalton Trans.(Themed issue on Small Molecules Activation) 45 (2016) 14419.
[9] N. Queyriaux, R.T. JaneJulien, M. Vincent, A.M. Chavarot-Kerlidou, Coord. Chem. Rev. 304 (2015) 3.
[10] B. Limburg, E. Bouwman, S. Bonnet, Coord. Chem. Rev. 256 (2012) 1451.
[11] D. Chatterjee, Coord. Chem. Rev. 16 (1998) 8273.
[12] D. Chatterjee, A. Mitra, G.S. De, Platinum Met. Rev. 50 (2006) 2.
[13] D. Chatterjee, R. van Eldik, Adv. Inorg. Chem. 64 (2012) 183.
[14] D. Chatterjee, R. van Eldik, Coord. Chem. Rev. 349 (2017) 129.
[15] D. Chatterjee, R. van Eldik, Macroheterocycles 13 (2020) 193.
[16] M.M. Taqui Khan, H.C. Bajaj, Z. Shirin, K. Venkatasubraminan, Ind. J. Chem(A) 31 (1992) 303.
[17] M.M. Taqui Khan, D. Chatterjee, R.R. Merchant, P. Paul, S.H.R. Abdi, M.R.H. Siddiqui, D. Srinivas, M.A. Moiz, M.M. Bhadbhade, K. Venkatasubraminan, Inorg. Chem. 31 (1992) 2711.
[18] T. Matsubara, C. Creutz, Inorg. Chem. 18 (1979) 1956.
[19] H.C. Bajaj, R. van Eldik, Inorg. Chem. 27 (1988) 4052.
[20] K. Shimizu, T. Matsubara, G.P. Sato, Bull. Chem. Soc. Jpn. 47 (1974).
[21] N. Oyama, F.A. Anson, J. Electroanal. Chem. 88 (1978) 289.
[22] M. Ikeda, K. Shimizu, G.P. Sato, Bull. Chem. Soc. Jpn. 55 (1982) 797.
[23] K. Shimizu, Bull. Chem. Soc. Jpn. 50 (1977) 2921.
[24] N. Oyama, F.A. Anson, J. Am. Chem. Soc. 101 (1979) 1634.
[25] T. Matsubara, C. Creutz, J. Am. Chem. Soc. 100 (1978) 6255.
[26] Y. Yoshino, T. Uehiro, M. Sato, Bull. Chem. Soc. Jpn. 52 (1979) 1060.
[27] L. Codognoto, P.G. Zanichelli, R.L. Sernaglia, J. Braz. Chem. Soc. 16 (2005) 620.
[28] R.B. Baar, F.C. Anson, J. Electroanal. Chem. 187 (1985) 265.
[29] P.G. Zanichelli, R.L. Sernagia, D.W. Franco, Langmuir 22 (2006) 203.
[30] P.G. Zanichelli, A.M. Miotto, H.F.G. Estrela, F.R. Soares, D.M. Grassi-Kassisse, R. C. Spadari-Bratfisch, E.E. Castellano, F. Roncarroli, A.R. Parise, J.A. Olabe, A.R.M. S. de Brito, D.W. Franco, J. Inorg. Biochem. 98 (2004) 1921.
[31] P.C.G. Benini, B.R. McGarvey, D.W. Franco, Nitric Oxide 19 (2008) 245.
[32] N.S. Scott, N. Oyama, F.C. Anson, J. Electroanal. Chem. 110 (1980) 303.
[33] M.M. Taqui Khan, K. Venkatasubramanian, Z. Shirin, M.M. Bhadbhade, J. Chem. Soc. Dalton Trans. (1995) 1031.
[34] R.C. Rocha, K. Araki, H.E. Toma, Transit. Met. Chem. 23 (1998) 13.
[35] R.C. Rocha, F.N. Rein, H.E. Toma, J. Braz. Chem. Soc. 12 (2001) 234.
[36] B.T. Khan, K. Annapoorna, Inorg. Chim. Acta 171 (1990) 157.
[37] A.A. Diamantis, J.V. Dubrawski, Inorg. Chem. 22 (1983) 1934.
[38] D. Chatterjee, H.C. Bajaj, A. Das, J. Chem. Soc. Dalton Trans. (1995) 2497.
[39] M.M. Taqui Khan, A. Hussain, M.A. Moiz, Polyhedron 11 (1992) 687.
[40] B.T. Khan, K. Annapoorna, Polyhedron 10 (1991) 2465.
[41] B.T. Khan, K. Annapoorna, Inorg. Chim. Acta 176 (1990) 241.
[42] D. Chatterjee, J. Mol. Catal (A): Chem. 127 (1997) 57.
[43] M.M. Taqui Khan, D. Chatterjee, M.R.H. Siddiqui, S.D. Bhatt, H.C. Bajaj, K. Venkatasubramanian, M.A. Moiz, Polyhedron 12 (1993) 1443.
[44] H.E. Toma, K. Araki, J. Coord. Chem. 24 (1991) 1.
[45] H.E. Toma, P.S. Santos, M.P.D. Mattioli, L.A.A. Oliveira, Polyhedron 6 (1987) 603.

[46] F.N. Rein, R.C. Rocha, H.E. Toma, J. Coord. Chem. 53 (2001) 99.
[47] H.E. Toma, M. Tsurumaki, J. Braz. Chem. Soc. 1 (1990) 17.
[48] F.N. Rein, R.C. Rocha, H.E. Toma, Electrochem. Commun. 4 (2002) 436.
[49] F.N. Rein, R.C. Rocha, H.E. Toma, J. Electroanal. Chem. 541 (2003) 103.
[50] K. Araki, F.N. Rein, S.G. Camera, H.E. Toma, Transit. Met. Chem. 17 (1992) 535.
[51] F.N. Rein, R.C. Rocha, H.E. Toma, J. Electroanal. Chem. 494 (2000) 21.
[52] M.M. Taqui Khan, K. Venkatasubramanian, Z. Shirin, M.M. Bhadbhade, J. Chem. Soc. Dalton Trans. (1992) 885.
[53] N.A. Ezerskaya, T.P. Solovykin, Z.h. Neorg, Khim. 11 (1966) 2179.
[54] N.A. Ezerskaya, T.P. Solovykin, Z.h. Neorg, Khim. 11 (1966) 2569.
[55] J. Zhou, W. Xi, J.K. Hurst, Inorg. Chem. 29 (1990) 160.
[56] I.A. Andrade de Oliveira, L.D. Ciana, A. Haim, Inorg. Chim. Acta 225 (1994) 129.
[57] A. Das, H.C. Bajaj, D. Chatterjee, Polyhedron 14 (1995) 3385.
[58] A. Das, H.C. Bajaj, Polyhedron 16 (1997) 1023.
[59] A.D. Shukla, H.C. Bajaj, A. Das, Angew. Chem. Int. Ed. 40 (2001) 446.
[60] A. Das, H.C. Bajaj, M.M. Bhadbadhe, J. Organomet. Chem. 544 (1997) 55.
[61] D. Chatterjee, A. Das, H.C. Bajaj, Inorg. Chem. 32 (1993) 4049.
[62] P. Forlano, F.D. Cukiernik, O. Polzat, J.A. Olabe, J. Chem. Soc. Dalton Trans. (1997) 1595.
[63] A. Das, H.C. Bajaj, Polyhedron 16 (1997) 3851.
[64] N.S. Hush, Prog. Inorg. Chem. 8 (1967) 391.
[65] Y. Dong, J.T. Hupp, Inorg. Chem. 31 (1992) 3322.
[66] D.E. Khoshtariya, H.C. Bajaj, P.A. Tregloan, R. van Edik, J. Phys. Chem. A 104 (2000) 5535.
[67] H.C. Bajaj, P.A. Tregloan, R. van Edik, Inorg. Chem. 43 (2004) 1429.
[68] L.B. Panice, E.A. de Oliveira, R.A.D. Molin Filho, D.P. de Oliveira, A.M. Lazarin, E. I.S. Andreotti, R.L. Sernaglia, Y. Gushikem, Mat. Sci. Eng. B 188 (2014) 78.
[69] R.C. Rocha, K. Araki, H.E. Toma, Inorg. Chim. Acta 285 (1999) 197.
[70] R.C. Rocha, H.E. Toma, Inorg. Chim. Acta 310 (2000) 65.
[71] H.C. Bajaj, A. Das, R. van Edik, J. Chem. Soc. Dalton Trans. (1998) 1563.
[72] M. Losada, J. Mol. Catal. 1 (1975) 245.
[73] M.R. Rhodes, M.H. Barley, T.J. Meyer, Inorg. Chem. 27 (1988) 4772.
[74] M.R. Rhodes, M.H. Barley, T.J. Meyer, Inorg. Chem. 30 (1991) 629.
[75] D. Chatterjee, S. Shome, N. Jaiswal, P. Banerjee, Dalton Trans. 43 (2014) 13596.
[76] Y. Chen, F.-T. Lin, R.E. Shepherd, Inorg. Chem. 38 (1999) 973.
[77] G. Ramachandraiah, J. Am. Chem. Soc. 116 (1994) 6733.
[78] R. Prakash, B. Tyagi, D. Chatterjee, G. Ramachandraiah, Polyhedron 16 (1997) 1235.
[79] I. Willner, D. Mandler, J. Am. Chem. Soc. 111 (1989) 1330.
[80] D. Chatterjee, N. Jaiswal, P. Banerjee, Eur. J. Inorg. Chem. (2014) 5856.
[81] J.P. Hoare, Standard potentials of oxygen, in: A.J. Bard, R. Persons, J. Jordan (Eds.), Standard Potentials in Aqueous Solutions, Dekker, New York, 1985, pp. 49–66.
[82] D. Chatterjee, N. Jaiswal, P. Sarkar, Dalton Trans. 44 (2015) 7613.
[83] E.J. Toone, Advances in enzymology and related areas of molecular biology, John Wiley and Sons, 2011.
[84] C. Song, J. Zhang, Electrocatalytic oxygen reduction reaction, in: J. Zhang (Ed.), PEM Fuel Cell Electrocatalyst: Fundamentals and Applications, Springer, London, 2008, pp. 89–134.
[85] D. Chatterjee, N. Jaiswal, A. Franke, R. van Eldik, Chem. Commun. 50 (2014) 14562.
[86] M. Wikström, K. Krab, V. Sharma, Chem. Rev. 118 (2018) 2469.
[87] Y.-W. Zhong, in: R.J. Mortimer, D.R. Rosseinsky, P.M.S. Monk (Eds.), Electrocromic materials and devices, Wiley-VCH Verlag GmbH & Co. KGaA, 2015, pp. 185–210, Chapter 6.